CDF/ANAL/EWK/CDFR/8539
December 5, 2006
Version 1.1

Search for WZ and ZZ Production in Multilepton Events Using 1.1 fb^{-1}

Shih-Chieh Hsu, Elliot Lipeles, Mark Neubauer, Rami Vanguri, Frank Würthwein

University of California, San Diego

Abstract

In this note, we present an analysis searching for WZ and ZZ production in multilepton events using 1.1 fb^{-1} of integrated luminosity. In the WZ analysis, we expect

$$9.75 \pm 0.03(stat.) \pm 0.31(syst.) \pm 0.59(lumi.)$$

events of signal and

$$2.65 \pm 0.28(stat.) \pm 0.33(syst.) \pm 0.09(lumi.)$$

We observe 16 WZ candidate events. Comparing a Maximum Likelihood fit in two bins of $\not\!\!E_T$ with expectations from background only, we find that 2 in a Billion background only experiments results in an ML fit significance as large as the one observed in data. This is equivalent to the one sided 5.9σ tail of a Gaussian distribution. This is the first observation ($> 5\sigma$) of WZ production.The measured cross section is

$$\sigma(WZ) = 5.0^{+1.8}_{-1.6}\ (\text{stat.} + \text{syst.})\ \text{pb}$$

consistent with the next to leading order SM prediction of 3.7 ± 0.3 pb. Both the cross-section and the two binned $\not\!\!E_T$ distribution used to assess the significance are consistent with the standard model expectations.

In the ZZ search, we expect

$$1.884 \pm 0.015\ (\text{stat.}) \pm 0.061\ (\text{syst.}) \pm 0.113\ (\text{lumi.})$$

events of signal and

$$0.009 \pm 0.007\ (\text{stat.}) \pm 0.004\ (\text{syst.}) \pm 0.0005\ (\text{lumi.})$$

events of background. We observe one 4 muon ZZ candidate, which corresponds to a 2.6 σ significance, based on which we set a limit of $\sigma(ZZ) < 3.8$ pb which is consistent with the NLO prediction of 1.39 ± 0.1 pb.

Contents

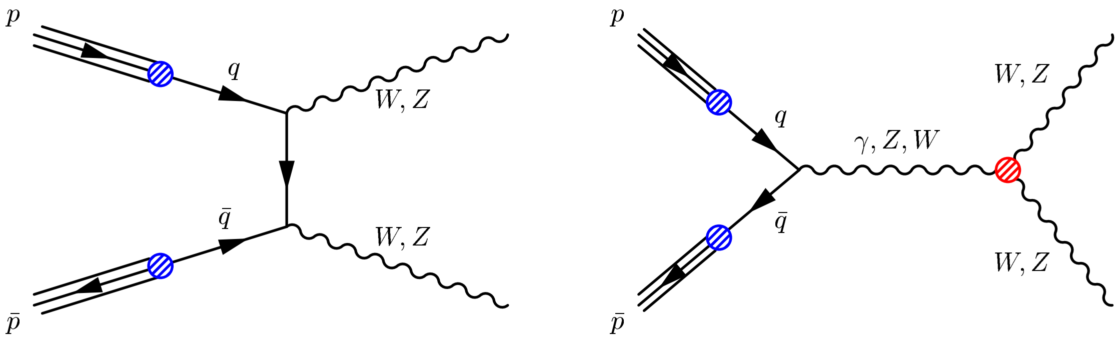

(a) t-channel

(b) s-channel, involving triple gauge boson coupling

Figure 1: Leading-order diagrams contributing to diboson production at the Tevatron.

1 Introduction

In $p\overline{p}$ collisions at the Tevatron, single W and Z bosons are copiously produced and extensively studied with the CDF detector. Diboson production is much more rare and, in fact, some final states have thus far not been conclusively observed (e.g. WZ). The production involves self-couplings of gauge bosons, often referred to as trilinear gauge couplings (TGCs), which are a rather striking consequence of the SU(2)$\otimes$U(1) structure of the Standard Model (SM). Detailed study of diboson production provides a stringent test of TGCs which are sensitive to new physics (NP) effects. Figure 1 shows the tree-level diagrams contributing to SM diboson production in $p\overline{p}$ collisons. As compared to LEP, diboson production at the Tevatron is sensitive to different coupling combinations (e.g. WWZ coupling via WZ final state and $WW\gamma$ coupling via $W\gamma$ final state) and higher q^2. The combination of both provides the Tevatron with sensitivity to new physics (NP) effects that can not be probed at LEP. In addition, Standard Model dibosons productionleads to final states which are very similar to NP signatures we search for at CDF and therefore represent important backgrounds to be understood. Turning this around, one could argue that observation of the more rare SM diboson final states (e.g. WZ$\rightarrow$trileptons or ZZ$\rightarrow$4 leptons) represents an important step in demonstrating our experimental sensitivity to NP signatures (e.g. SUSY $\tilde{\chi}_1^{\pm}\tilde{\chi}_2^0$ production) involving multileptons and/or missing transverse energy ($\not\!\!E_T$).

In this note, we present analyses searching for WZ and ZZ production using 1fb^{-1} of integrated luminosity. Our search is for $WZ \rightarrow 3\ e, \mu$ leptons + $\not\!\!E_T$ and $ZZ \rightarrow 4\ e, \mu$ leptons. The diagrams for WZ and ZZ are shown in Figure 2, along with a breakdown of the final states resulting from their decay. Measurement of WZ production can be used to make a model-independent test of the WWZ Standard Model gauge coupling via the

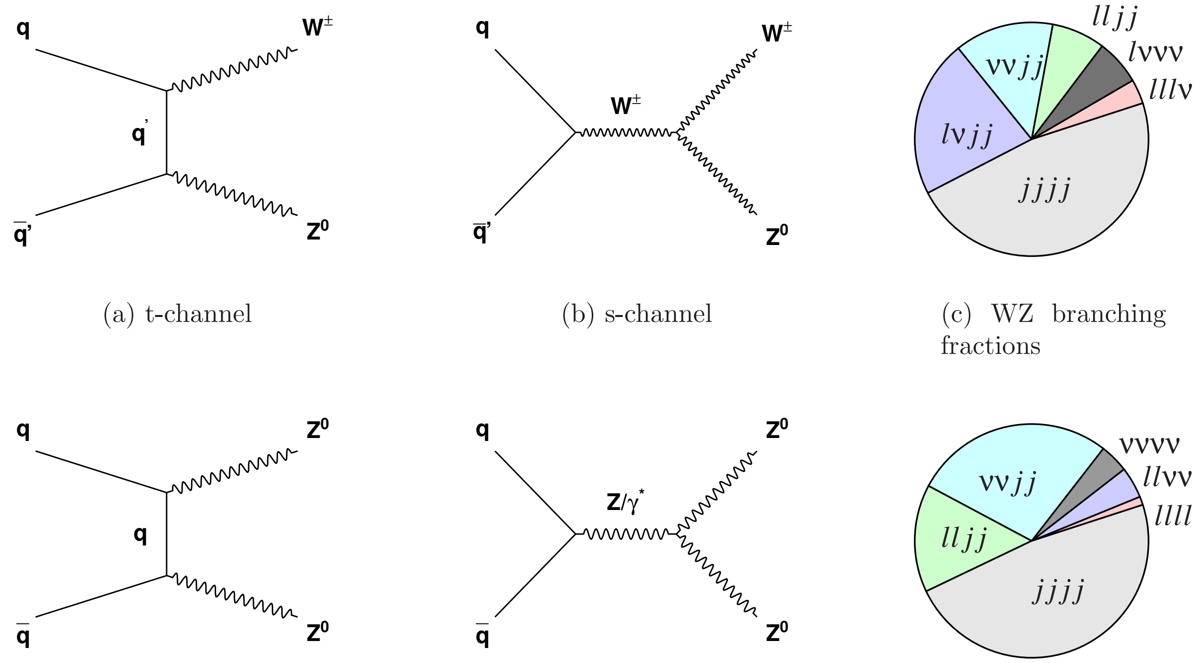

(a) t-channel

(b) s-channel

(c) WZ branching fractions

(d) t-channel

(e) s-channel

(f) ZZ branching fractions

Figure 2: Leading-order diagrams contributing to WZ,ZZ production at the Tevatron and fractions decaying to final states involving leptons and jets. The branching fraction of $WZ \to 3\ e, \mu$ leptons is 1.8%. The branching fraction of $ZZ \to 4\ e, \mu$ leptons is 0.5%

diagram shown in Figure 2(b). The s-channel diagrams shown in Figure 2(e) involving γZZ and ZZZ TGCs are identically zero in the SM since neither the Z nor γ carry charge or weak isospin to which the gauge bosons couple. Significant enhancement of the observed cross section above the SM prediction for ither WZ or ZZ would represent evidence for NP. In the absense of such evidence, limits on anomalous TGC couplings can be derived.

The NLO total cross section for WZ and ZZ production at $\sqrt{s} = 1.96$ is 3.7 ± 0.1pb and 1.4 ± 0.1, respectively [1]. CDF published [2] a search for the sum of WZ and ZZ production in 2, 3, and 4 lepton channels using 194pb^{-1} of integrated luminosity and set a limit of $\sigma(p\bar{p} \to WZ + ZZ) < 15.2$pb at 95% C.I.

The analyses presented in this note build upon work documented in [3] and references therein. In this previous analysis, a search for WZ production in $WZ \to 3\ e, \mu$ leptons + $\not\!\!E_T$ using 825pb^{-1} resulted in two events observed (both eee) with an expected signal of 3.7 ± 0.3 events and expected background of 0.9 ± 0.2 events. These results are consistent with both background-only and background+signal expectations and an upper limit of $\sigma(p\bar{p} \to WZ) < 6.34$pb at 95% C.I. was determined. The primary improvements in the current analysis over our previous WZ analysis are:

- Addition of new lepton categories (selections), roughly doubling the signal acceptance.
- Including MET+PEM trigger.
- Addition of all data currently available (+35%)

In addition, we have added a search for SM ZZ production in $ZZ \to 4\ e, \mu$ using the new set of leptons and the full dataset.

2 Event Selection

In this section, we describe our candidate selection. This includes the trigger datasets we use in our analysis, reconstruction of low-level objects used in the selection, and our high-level cuts.

2.1 Strategy

Our strategy is to search for WZ candidates which decay to three final state leptons with missing large transverse energy ($\not\!\!E_T$). The signal $\not\!\!E_T$ is primarily from the neutrino energy in W $\to$ eν and W $\to$ $\mu\nu$ decay with possibly additional contributions from leptonic τ decays. For the ZZ analysis, we search for candidates with four leptons and with no requirement on the $\not\!\!E_T$. In both cases, we require that there be at least two opposite charge, same flavor leptons with invariant mass near the Z mass, consistent with coming from Z decay. We require one lepton to be consistent with having generated one of the high p_t inclusive lepton triggers and allow for the other leptons in the event to be identified but loosely selected and have momentum below the trigger threshold.

Using this selection, the dominant WZ backgrounds are from Z+X, with X $\equiv$ Z, γ, or jet(s) reconstructed as an identified lepton. The only background expected to contribute at any significant level in the ZZ selection is Z+di-fake.

2.2 Datasets

We use the high p_t inclusive lepton triggers for our analysis. Specifically, we use the following four trigger paths:

- ELECTRON_CENTRAL_18
- MUON_CMUP18
- MUON_CMX18
- MET_PEM (WZ only)

The corresponding datasets are bhel0d/0h/0i (electrons), bhmu0d/0h/0i (muons), and bpel0d/0h/0i (MET+PEM). We only include runs in the following v13 good run lists:

- EM_NOSI
- EM_CMUP_NOSI
- EM_MU_NOSI_CMXIGNORED
- EM_SI
- EM_CMUP_SI
- EM_MU_SI_CMXIGNORED

The luminosity of each good run list is shown in Table 2.2.

2.3 Low-level Objects

Selection begins with construction of categories of identified leptons, reconstruction of jets and calculation of the $\not\!\!E_T$ in each event. These are described in the present section.

Good run list	$\mathcal{L}$ (pb^{-1})
EM_NOSI	1100.9
EM_CMUP_NOSI	1078.7
EM_MU_NOSI_CMXIGNORED	1030.5
EM_SI	1019.6
EM_CMUP_SI	997.7
EM_MU_SI_CMXIGNORED	954.6

Table 1: Luminosity for each of the good run lists (v13) used in this analysis. These have been scaled by the factor of 1.019.

2.3.1 Lepton Identification and Categories

We use a total of nine categories of leptons for this analysis, four categories of identified electrons and muons each, and a "Crack Track" category. The electrons are TCE, LCE, PHX, and PEM, where LCE is a significantly loosened version of the TCE cuts, PHX are plug electrons with a Pheonix track, and PEM are plug electrons without an associated Pheonix track. The muons are CMUP, CMX, CMIOCES, and CMIOPES where CMIOCES (CMIOPES) is defined as a cental (plug) track object that passes the MIP selection, but does not pass the CMUP and CMX selection. In addition, we consider a "Crack Track" lepton (CrkTrk) which is not track CES or PES fiducial and also does not pass the CMUP or CMX selection. The electron, muon, and CrkTrk selection criteria are detailed in Tables 2-6.

These categories all extend down to 10 GeV E_T, but we require at least one $E_T >$ 20 GeV lepton for triggering. This choice and the use of standard TCE, CMUP, CMX, and PEM selections means that the trigger efficiencies measured in [4]-[5] and shown in Table 7 are applicable.

The coverage in $\eta - \phi$ space for leptons used in this analysis and the leptons used in the previous analysis is shown in Figures 3(a),4(a) and 3(b),4(b), respectively.

2.3.2 Jets

Jets are used as part of the $\not\!\!E_T$ correction. The jets used in this correction are selected with a cone size of ΔR <0.4 based on the JetClu algorithm. The latest level 5 corrections[1] are used to correct the absolute energy scale of the jets, but the higher level out of cone and underlying event corrections are not applied in order to avoid double counting or under counting of the energy. For purposes of jet counting, we do not count jets within $\Delta R < 0.4$ of our reconstructed leptons.

[1]based upon the jetCorr06b tag of JetUser package

	TCE/LCE
Region	Central
Fiducial	Track Fiducial to CES
Track p_T	$>= 10(5 \text{ if } \mathrm{E_t} < 20)$
Track $\lvert z_0 \rvert$	$<= 60$ cm
#Ax SL (5hits)	$>= 3$
#St SL (5hits)	$>= 2$
Conversion	$! = 1$
Had/Em	$<= 0.055 + 0.00045E$
Iso/E_T	$<= 0.1$
Lshr	$<= 0.2$
E/P	$< 2.5 + 0.015 * E_T$
Signed CES ΔX	$-3 <= q\Delta X <= 1.5$ cm
$CES\lvert\Delta Z\rvert$	< 3 cm
Tracks	BcTrk (Larry's Correction if Data)

Table 2: Selection for central leptons. TCE candidates are the full table and LCE is same as TCE with the cuts in red (in the second box) removed.

	PHX/PEM
Region	Plug
Pes2DEta	$1.2 < \lvert\eta\rvert < 2$ (2.8 PEM)
Had/Em	$<= 0.05$
PEM3x3FitTower	true
$PEM3x3\chi^2$	$<= 10$
Pes5x9U	$>= 0.65$
Pes5x9V	$>= 0.65$
Iso/Et	$<= 0.1$
ΔR(Pes,PEM)	$<= 3.0$
PHX only	
Track Match	True
NSiHits	$>= 3$
Track $\lvert Z0\rvert$	$<= 60cm$
PEM	Not above PHX track requirements

Table 3: Selection for phoenix (PHX) and trackless (PEM) plug electrons

	CMUP/CMX
CMU Fid	x-fid< 0 cm z-fid< 0cm
CMP Fid	x-fid< 0 cm z-fid<-3cm
CMX Fid	x-fid< 0 cm z-fid<-3cm
E_{em}	$<= 2 + max(0, (p - 100) * 0.0115)$
E_{had}	$<= 6 + max(0, (p - 100) * 0.028)$
Iso/Pt	$<= 0.1$
NAxL(5 hits)	$>= 3$
NStL(5 hits)	$>= 2$
Track $\|Z_0\|$	$<= 60cm$
Track $\|D_0\|$	$<= 0.2cm$ (0.02cm if NSiHit> 0)
χ^2/dof	$<= 4$ (3 if run $<= 186598$)
$\|\Delta X_{CMU}\|$	$<= 7cm$
$\|\Delta X_{CMP}\|$	$<= 5cm$
$\|\Delta X_{CMX}\|$	$<= 6cm$
ρ_{exit}	> 140 cm if CMX
CMP veto	No Bluebeam in CMP for run < 154449
CMX veto	No CMX for run < 150144, No Miniskirt, No Keystone
Arches	Arches only for all run range
	Arches removing wedge 14 on West Side for run > 190697
Tracks	BcTrk (Larry's Correction if Data)

Table 4: Selection for CMUP and CMX muons

	CMIOCES/CMIOPES
E_{em}	$<= 2 + max(0, (p - 100) * 0.0115)$
E_{had}	$<= 6 + max(0, (p - 100) * 0.028)$
Iso/Pt	$<= 0.1$
Uniqueness	Not a CMUP or CMX muon
Track $\lvert Z_0 \rvert$	$<= 60cm$
Track $\lvert D_0 \rvert$	$<= 0.2cm$ (0.02cm if NSiHit$>$ 0)
$E_{em} + E_{had}$	$> 0.1GeV$
Central	Track CES Fiducial
NAxL(5 hits)	$>= 3$
NStL(5 hits)	$>= 3$
χ^2/dof	$<= 3$
	BcTrk (Larry Correction if Data)
Forward	Track PES Fiducial
Cot Hit Fraction	> 0.6
	No beam constriant on IO tracks

Table 5: Selection for CMIOCES and CMIOPES

	CrkTrk
Iso/Pt	$<= 0.1$ using CDF Muon *or*
	$<= 0.1$ using nearest CDF EMObj with $\Delta R < 0.05$
Track $\lvert Z_0 \rvert$	$<= 60cm$
Track $\lvert D_0 \rvert$	$<= 0.2cm$ (0.02cm if NSiHit$>$ 0)
χ^2/dof	$<= 3$
NAxL(5 hits)	$>= 3$
NStL(5 hits)	$>= 3$
Uniqueness	Not a CMUP or CMX muon
Is in Crack	Not Track CES or PES Fiducial
Conversion	$! = 1$
	BcTrk (Larry Correction if Data)

Table 6: Selection for CMIOCES and CMIOPES

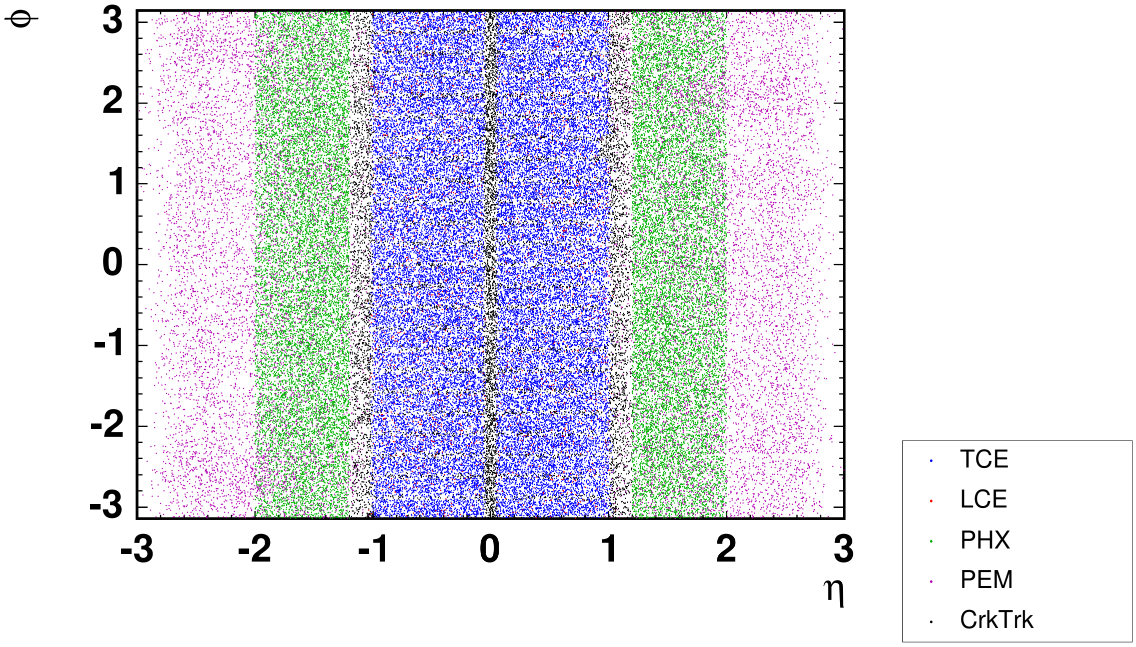

(a) New electron categories

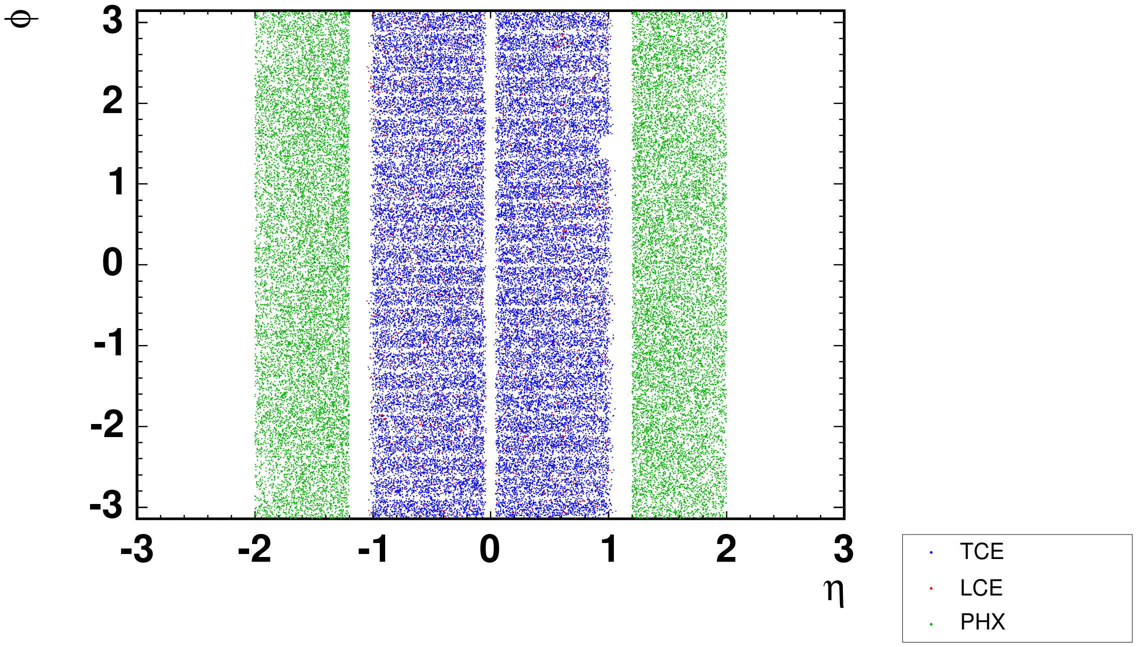

(b) Old electron categories

Figure 3: Comparision of the coverage of the new and old electron categories.

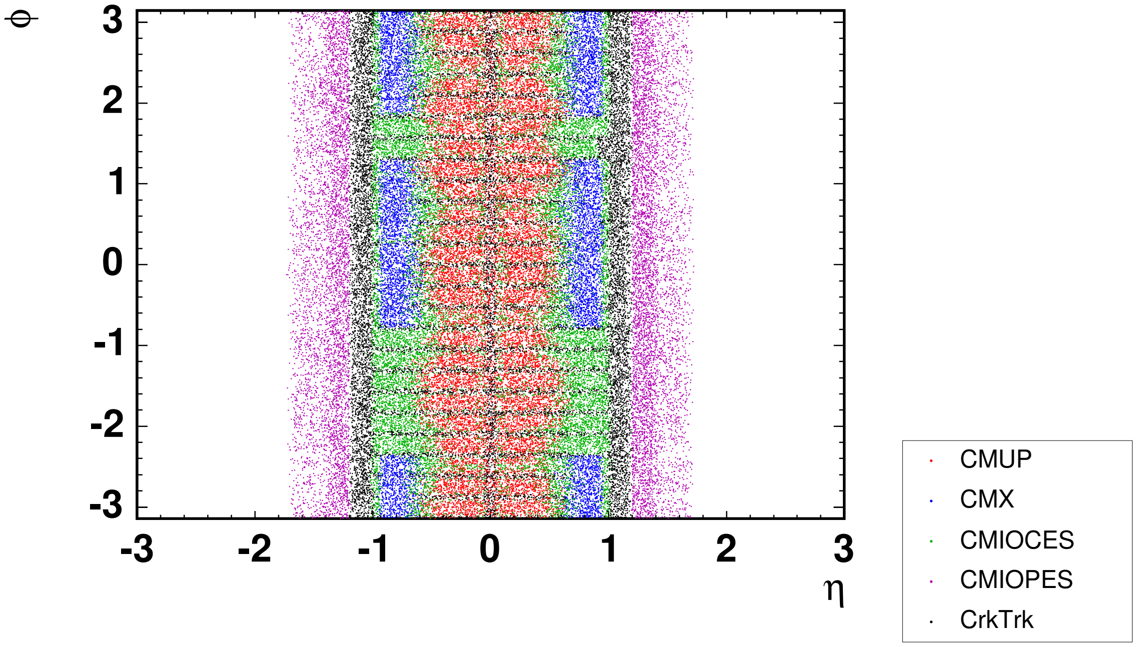

(a) New muon categories

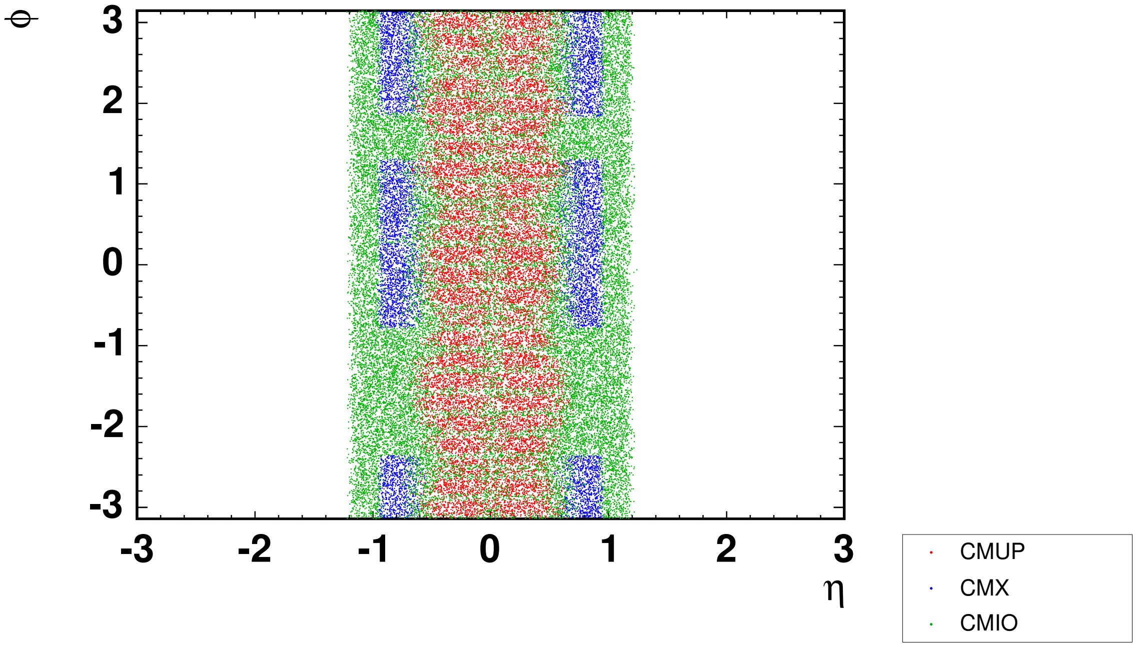

(b) Old muon categories

Figure 4: Comparision of the coverage of the new and old muon categories.

	Gen5	Gen6	CDF Note
TCE	0.9620 ± 0.006	0.9766 ± 0.006	7939
PHX/PEM	0.910 ± 0.003	0.910 ± 0.003	7940
CMUP	0.8977 ± 0.005	0.9186 ± 0.004	7956
CMX	0.9665 ± 0.004	0.9586 ± 0.004	7956

Table 7: Triggerable lepton types and the trigger effieciencies used in this analysis. Note that PHX/PEM shown in an average. We use the full turn on curve as a function of E_T, η, and $\not\!\!E_T$ for the MET+PEM trigger.

2.3.3 Missing Transverse Energy ($\not\!\!E_T$)

The $\not\!\!E_T$ calculation used for this analysis starts with the sum of the transverse energy over the entire calorimeter using the highest $\sum p_T$ vertex to define the directions. The $\not\!\!E_T$ is then corrected for the identified muons by subtracting the muons p_T and adding back its calorimeter E_T. Finally the $\not\!\!E_T$ is corrected for jets $E_T > 15$ GeV and $|\eta| < 2.5$ which do not $\Delta R < 0.4$ match any identified leptons in the event, by subtracting the corrected jet E_T and adding back the raw E_T.

2.4 High-level Cuts

This section describes the high-level cuts we make in our WZ and ZZ candidate selection. We require there to be 3 (4) and only 3 (4) reconstructed leptons passing our lepton identification cuts for WZ (ZZ) analyses. We do not make any selection on the number of jets in the event, as $t\bar{t}$ background is expected to be small for both analyses.

2.4.1 Cosmic Rays (both WZ and ZZ analyses)

To reject cosmic ray events contaminating our muon candidates, we veto events tagged as di-cosmic by the CosmicFinderModule. This is equivalent to requiring the HasNotOutgoingPair $! = 1$ from the TStnCosmicBlock in Stntuple.

2.4.2 Δz_0 (both WZ and ZZ analyses)

We require that the z_0 of the tracks for the lepton candidate be sufficiently close to each other because the diboson events we are searching for have decay daughters that originate from a common vertex. This reduces contamination from poorly reconstructed tracks, cosmics, multiple interactions, etc. Our selection requires that the maximum Δz_0 between pairs of our trilepton candidate be less than 4 cm. Since the PEM lepton category has no associated track, the PEM leptons are excluded from the Δz_0 calculation. This

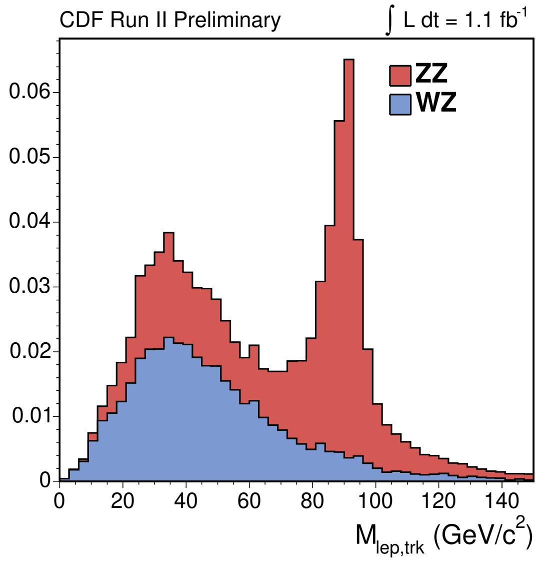

Figure 5: MlepTrk in WZ signal region

cut accepts >99.5% of the WZ and ZZ signal based upon our reconstructed PYTHIA samples.

2.4.3 Z Mass Region (both WZ and ZZ analyses)

Since we are searching diboson states involving a Z, we require there be at least two opposite charge, same flavor leptons with invariant mass near the Z mass, consistent with having originating from Z decay. Since we expect the dominant backgrounds to involve a decay of Z boson, we are actually not very sensitive to the choice of Z mass window in the WZ and ZZ analyses. We choose a Z mass window of ($76 < \mathrm{M}_{\mathrm{l}^+\mathrm{l}^-} < 106$ GeV) which the same used in the previous WZ(+ZZ) analysis[6].

2.4.4 ZZ Veto (WZ analysis only)

The decay of ZZ where both Z bosons decay to charged leptons can enter our trilepton selection when one of the leptons does not pass our identification cuts. A HEPG study of ZZ decays reconstructed in the trilepton mode shows that there are three main cases (i) decays involving τ's where one τ decays leptonically and the other hadronically (ii) lepton falls into region where we do not have ID acceptance but do have tracking acceptance (e.g. crack), and (iii) same as (ii) but we have neither id nor track acceptance (e.g. forward muons). For (ii), we can recover these as ZZ background by looking for one or more additional tracks ($\mathrm{p_t} > 8$ GeV, standard d_0, z_0 cuts) which make a Z mass ($76 < \mathrm{M}_{\mathrm{l}^+\mathrm{l}^-} <$ 106 GeV) with the lepton not involved in making the Z region cut previously mentioned. We find this cut reduces the ZZ background by $\sim$40% with negligible effect on the WZ signal.

2.4.5 $\not\!\!E_T$ (WZ analysis only)

$\not\!\!E_T$ is the most powerful high-level cut for removing backgrounds from the WZ search region. As with the previous analysis, we require $\not\!\!E_T > 25$ GeV in our event selection.

2.4.6 $\Delta\phi(\not\!\!E_T, \text{lepton}, \text{jet})$ (WZ analysis only)

Since the dominant backgrounds are at low $\not\!\!E_T$ and mis-measured $\not\!\!E_T$ is correlated to the direction of leptons and/or jets in the event, we require $\Delta\phi(\not\!\!E_T, \text{lepton}, \text{jet}) > 0.16$ (rad), where $\Delta\phi(\not\!\!E_T, \text{lepton}, \text{jet})$ is the ϕ angle between the $\not\!\!E_T$ and the nearest lepton or jet in the event.

3 Signal and Background Expectations

In this section, we present the expected signal and background acceptances for the WZ and ZZ analyses.

3.1 Monte Carlo Samples

The geometric and kinematic acceptance for signal and backgrounds (except fakes) are determined from Monte Carlo using a full GEANT-based simulation of the detector.

3.1.1 Heavy dibosons: WW, WZ, ZZ

The WZ and ZZ samples we use are based upon the PYTHIA event generator. The WZ samples are decayed with the Z decaying to a pair of e, μ, or τ leptons, and the W decaying generically, which is then filtered for two e or μ leptons above 1 GeV. The ZZ sample is constructed with both Z's decaying generically and then filtered for two e or μ leptons above 1 GeV. The ZZ Monte Carlo includes γ^* component (and simulates the interference) and has an $\mathrm{M_Z} > 15$ GeV generator-level requirement.

3.1.2 $Z\gamma$

The $Z\gamma$ Monte Carlo used for this analysis uses the Baur matrix element generator [7] which is passed to PYTHIA via the LesHouchesModule. Because of some indecision over the proper settings for the PYTHIA QED radiation settings the Gen5 sample has the QED turned off and the Gen6 sample has it turned on. In both the $Z\gamma \to ee\gamma$ and $Z\gamma \to \mu\mu\gamma$ samples, the QED radiation setting in PYTHIA was turned off. Effects from QED radiation are small for this analysis compared to uncertainties from the conversion finding efficiency and K-factor uncertainties.

3.1.3 $t\bar{t}$

The $t\bar{t}$ sample is generated at a mass of 175 GeV, uses Gen5 for the full run range and has no minbias in the events. The NLO cross section is 6.7±0.7 pb.

3.1.4 $Z \to ee$ and $Z \to \mu\mu$

The $Z \to ee$ and $Z \to \mu\mu$ samples are generated with a 20 GeV minimum dilepton mass. They use Gen5 for the 0d run range and Gen6 for the 0h run range. They have a full luminosity dependent addition of minbias in the events.

3.2 Acceptance calculation

Determinaton of the acceptance is made separately for each of our trilepton categories. Each category is corrected for the lepton identification scale factors and trigger efficiencies that are relevant to that specific trilepton category and for the relative luminosity of applicable good run list to the EM_NOSI good run list. The master formula is then

$$A_i \quad = \quad \frac{N_{\mathrm{reco}}}{N_{\mathrm{gen}}(|Z_0| < 60 \text{ cm})} \times \epsilon_{trg} \times s_{lep} \times \epsilon_{vtx} \times \frac{\mathcal{L}_i}{\mathcal{L}_{\mathrm{em\_nosi}}} \tag{1}$$

where $A\epsilon$ is the acceptance times the efficiency and

- N_{reco} is the number of reconstructed events passing the full selection,
- $N_{\mathrm{gen}}(|Z_0| < 60 \text{ cm})$ is the number of generated events with 60 cm of the interaction point
- ϵ_{trg} is the effective trigger efficiency for the category (see below),
- s_{lep} is the effective lepton id scale factor (see below),
- ϵ_{vtx} is $0.9555 \pm 0.0004(stat) \pm 0.0031(sys)$ from CDF note 7935, and
- $\frac{\mathcal{L}_i}{\mathcal{L}_{\mathrm{em\_nosi}}}$ accounts for the relative amount of the applicable good run list.

3.2.1 Lepton Id Scale Factors

The lepton id scale factors and uncertainties for electrons and muons are summarized in Tables 8 and 9. They are discussed in detail in [8]. These are applied by simply multiplying together the scale factor for each lepton type assuming that they are completely uncorrelated.

Lepton Type	Data	MC	Scale Factor
0d			
TCE	0.876 ± 0.004	0.861 ± 0.001	1.017 ± 0.005
LCE	0.918 ± 0.003	0.906 ± 0.001	1.013 ± 0.003
PHXTrk	0.864 ± 0.004	0.866 ± 0.001	0.998 ± 0.005
PHXPEM	0.850 ± 0.005	0.894 ± 0.001	0.951 ± 0.006
PEM	0.805 ± 0.009	0.856 ± 0.002	0.940 ± 0.011
CrkTrk e	0.784 ± 0.012	0.835 ± 0.002	0.939 ± 0.015
0h			
TCE	0.865 ± 0.003	0.860 ± 0.001	1.006 ± 0.004
LCE	0.907 ± 0.003	0.902 ± 0.000	1.006 ± 0.003
PHXTrk	0.881 ± 0.003	0.872 ± 0.001	1.010 ± 0.004
PHXPEM	0.836 ± 0.004	0.879 ± 0.001	0.951 ± 0.005
PEM	0.758 ± 0.007	0.825 ± 0.001	0.919 ± 0.009
CrkTrk e	0.830 ± 0.011	0.862 ± 0.001	0.963 ± 0.013
0i			
TCE	0.866 ± 0.006	0.860 ± 0.001	1.007 ± 0.007
LCE	0.906 ± 0.006	0.902 ± 0.000	1.004 ± 0.007
PHXTrk	0.883 ± 0.006	0.872 ± 0.001	1.013 ± 0.007
PHXPEM	0.819 ± 0.008	0.879 ± 0.001	0.932 ± 0.009
PEM	0.739 ± 0.016	0.825 ± 0.001	0.896 ± 0.019
CrkTrk e	0.813 ± 0.023	0.862 ± 0.001	0.943 ± 0.027

Table 8: Lepton ID scale factors for electrons

Lepton Type	Data	MC	Scale Factor
0d			
CMUPId	0.939 ± 0.009	0.926 ± 0.001	1.014 ± 0.010
CMUPReco	0.921 ± 0.007	0.975 ± 0.001	0.945 ± 0.007
CMXId	0.940 ± 0.012	0.922 ± 0.002	1.020 ± 0.013
CMXReco	1.001 ± 0.008	0.999 ± 0.001	1.002 ± 0.008
CMIOCES	0.853 ± 0.013	0.818 ± 0.002	1.043 ± 0.016
CMIOPES	0.897 ± 0.009	0.893 ± 0.002	1.004 ± 0.010
CrkTrk μ	0.824 ± 0.011	0.876 ± 0.002	0.941 ± 0.013
0h			
CMUPId	0.918 ± 0.006	0.925 ± 0.001	0.992 ± 0.007
CMUPReco	0.913 ± 0.006	0.975 ± 0.001	0.936 ± 0.006
CMXId	0.918 ± 0.010	0.922 ± 0.002	0.996 ± 0.011
CMXReco	1.003 ± 0.009	0.998 ± 0.001	1.005 ± 0.009
CMIOCES	0.846 ± 0.010	0.817 ± 0.001	1.035 ± 0.012
CMIOPES	0.877 ± 0.008	0.885 ± 0.001	0.991 ± 0.009
CrkTrk μ	0.886 ± 0.008	0.907 ± 0.001	0.977 ± 0.009
0i			
CMUPId	0.906 ± 0.013	0.925 ± 0.001	0.979 ± 0.014
CMUPReco	0.918 ± 0.012	0.975 ± 0.001	0.942 ± 0.012
CMXId	0.926 ± 0.018	0.922 ± 0.002	1.004 ± 0.020
CMXReco	1.013 ± 0.014	0.998 ± 0.001	1.015 ± 0.014
CMIOCES	0.842 ± 0.019	0.817 ± 0.001	1.031 ± 0.023
CMIOPES	0.870 ± 0.017	0.885 ± 0.001	0.983 ± 0.019
CrkTrk μ	0.870 ± 0.015	0.907 ± 0.001	0.959 ± 0.017

Table 9: Lepton ID scale factors for muons

	Acceptance	Expected Yield
WZ		
e e e	(2.726 ± 0.015)%	1.972 ± 0.011
e e μ	(2.205 ± 0.014)%	1.595 ± 0.010
e μ μ	(1.753 ± 0.012)%	1.268 ± 0.009
μ μ μ	(1.391 ± 0.011)%	1.006 ± 0.008
e e t	(1.901 ± 0.013)%	1.375 ± 0.009
e μ t	(1.545 ± 0.011)%	1.117 ± 0.008
μ μ t	(1.138 ± 0.010)%	0.823 ± 0.007
e t t	(0.452 ± 0.006)%	0.327 ± 0.004
μ t t	(0.255 ± 0.005)%	0.185 ± 0.003
Total	(13.367 ± 0.034)%	9.668 ± 0.024

Table 10: WZ signal acceptance and expected yields.

3.2.2 Trigger Efficiencies

The trigger efficiencies are applied using the expression:

$$\epsilon_{trg} = 1 - (1 - \epsilon_{trg}^{\text{leg } 1}) \times (1 - \epsilon_{trg}^{\text{leg } 2}) \times (1 - \epsilon_{trg}^{\text{leg } 3})[\times(1 - \epsilon_{trg}^{\text{leg } 4})] \tag{2}$$

where $\epsilon_{trg}^{\text{leg } 1,2,3,4}$ are the trigger efficiencies for each leg. If one leg is not triggerable then its efficiency is set to zero. In order to count as a triggerable leg, the leg must satisfy the TCE, CMUP, CMX, PHX, or PEM lepton criteria with $\mathrm{E_t} > 20$ GeV and match to a L3 trigger object.

3.3 Signal

Table 10 shows the fraction of generated WZ→ 3 e, μ leptons (including e, μ leptons from τ's) that pass our selection cuts. It also shows the expected WZ signal yield for the full dataset after selection cuts. Table 11 shows the expected ZZ yield for each flavor channel in the ZZ search analysis. In the case of ZZ, we require there to be at least two pairs of same-flavor opposite sign leptons with one pair having mass within (76,106) and the other pair within (40, 140) GeV.

3.4 Backgrounds

We estimate the backgrounds to our WZ signal using a combination of Monte Carlo and data. The acceptance for ZZ, Zγ and $t\bar{t}$ backgrounds are determined from the Monte Carlo samples and scaled by the appropriate factors for cross section × branching fraction, filter

	Expected Yield
Category	ZZ
e e e e	0.280±0.006
e e e μ	0.000±0.000
e e μ μ	0.427±0.007
e μ μ μ	0.000±0.000
μ μ μ μ	0.186±0.005
e e e trk	0.207±0.005
e e μ trk	0.210±0.005
e μ μ trk	0.153±0.004
μ μ μ trk	0.174±0.004
e e trk trk	0.080±0.003
e μ trk trk	0.073±0.003
μ μ trk trk	0.070±0.003
e trk trk trk	0.012±0.001
μ trk trk trk	0.011±0.001
Total	1.884±0.015

Table 11: ZZ expected yield.

efficiency, and luminosity to arrive at expected yields corresponding to our dataset and selection. The background due to jet fakes are determined from data. The ZZ search analysis, the only background found to contribute is Z+jets.

3.4.1 ZZ

The ZZ process contributes to our trilepton sample when each Z decays leptonically and either one of the e,μ leptons is not identified or a generated τ from a Z decays hadronically. Recall that the former situation is mitigated by searching for an isolated track in addition to our reconstructed trileptons which makes a Z mass with the lepton remaining after the opposite-sign same-flavor Z selection.

We use the `wewk7d` PYTHIA MC sample to generate our ZZ acceptance and event yield expectations. In the case of ZZ, PYTHIA includes the γ^* component for each Z and simulates the interference between the two. Therefore, a simple counting of the fraction of reconstructed trileptons from generated events underestimates the background. To account for the γ^* component in the cross-section, we have run MCFM to calculate the NLO cross section with the $\gamma*$ component and M(Z)>15 GeV to be 2.116 pb.

The total background from ZZ is estimated to be 0.89 ± 0.01 events.

3.4.2 Zγ

The Zγ mode enters our selection when the photon is reconstructed as an electron and we also have large $\not\!\!E_T$. This is usually due to a conversion. In the central electron selections, we explicitly veto conversions, but the efficiency of this veto may not be well modeled in the Monte Carlo. In CDF Note 8073[9] Attal et al. measure a conversion veto scale factor by identifying conversions using the CES and then determining the rate at which they are vetoed. For the energy range $E_T > 10$ GeV, they find a scale factor of $\approx 1.3 \pm 0.1$. In the plug region, the conversion rate is sensitive to the material description in the Monte Carlo which is not tuned perfectly.

Based on the conversion veto scale factor, we scale the $Z\gamma$ up by 1.3. The total background from Zγ is estimated to be 0.03 ± 0.01 events from the sum of $Z\gamma \rightarrow \mu\mu\gamma$ and $Z\gamma \rightarrow ee\gamma$ contributions.

3.4.3 $t\bar{t}$

In the trilepton channel, $t\bar{t}$ is expected be a small background so we do not make a jet multiplicity requirement ($t\bar{t}$ contributes mainly to $N_{jets} \geq 2$.) The total background from $t\bar{t}$ is estimated to be 0.12$\pm$0.01 events.

3.4.4 Fakes from Z+jets

The WZ$\rightarrow$ trilepton signal has a background from the Z+jet(s) process when one of the jets is reconstructed as identified lepton. The lepton fake probabilities ("rates") are measured in the inclusive jet samples after corrections are made for small contributions from real isolated leptons from electroweak processes. The details of this determination and application of the fake rates to obtain fake background yields are described in CDF Note 8093[10], so we only summarize them here.

The fakes rate for each type of lepton is shown in Figures 6-3.4.4. These represent the probability of a loosely selected "lepton" (sufficiently looser than the full ID, referred to as "denominator objects" or "fakeable objects") in a jet to be identified as real lepton in our reconstruction. Tables 12-13 detail the denominators definition we use in our analysis.

The fake rates are applied to the data by selecting events with same event selection criteria as the signal selection, except that one of leptons is a denominator object. For each numerator type that the denominator could fake, a candidate is generated and weighted with the fake rate for that numerator type. For example a FakeableMuonCentral that is fiducial to the CMUP and CMIOCES could fake either a CMUP or a CMIOCES, so both possibilities are accounted for.

For this proceedure, one of the dileptons is required to pass the trigger criteria. It is possible however to trigger on a fake lepton, so we correct for the fraction of dilepton+fake events where only the fake is a triggerable object with Monte Carlo. This is done by

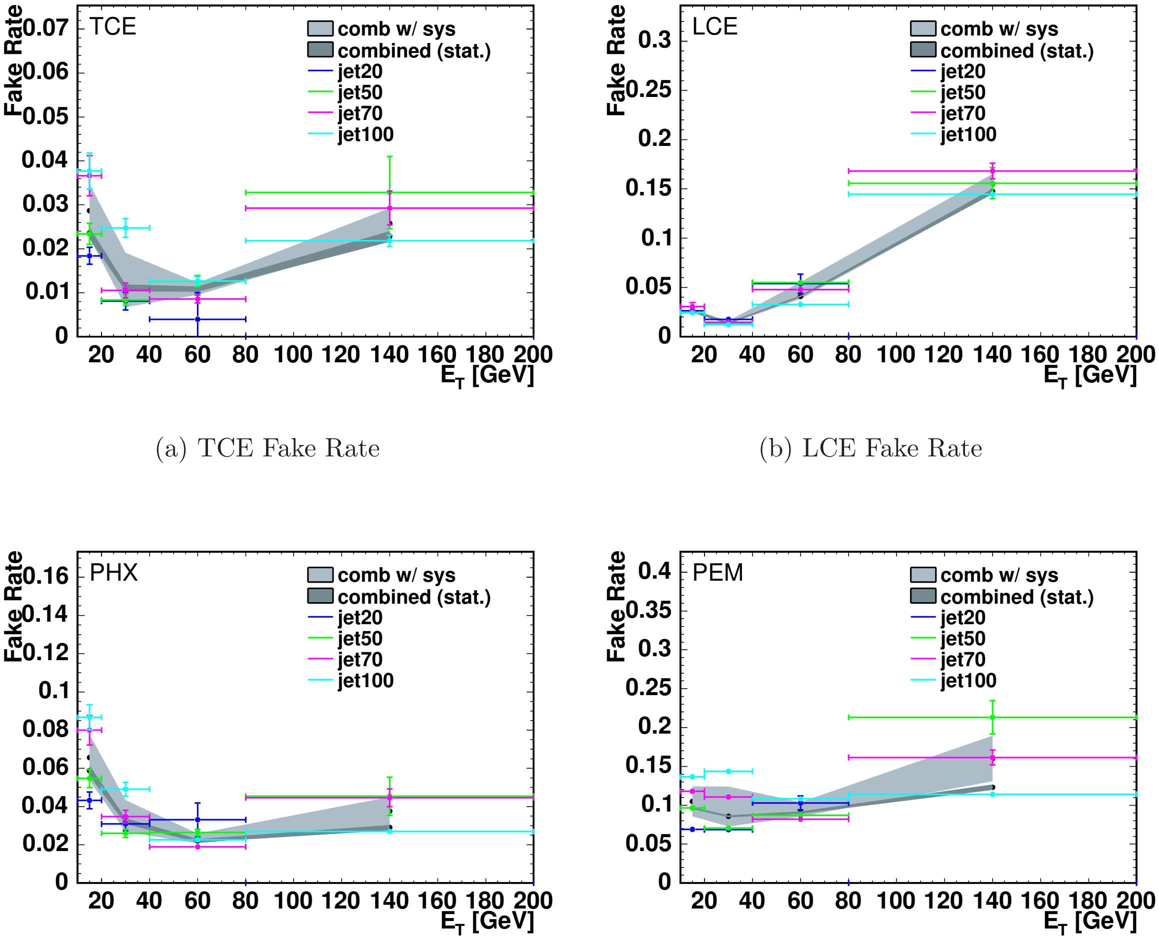

(a) TCE Fake Rate

(b) LCE Fake Rate

(c) PHX Fake Rate

(d) PEM Fake Rate

Figure 6: Jet $\rightarrow$ lepton fake rates for electron types

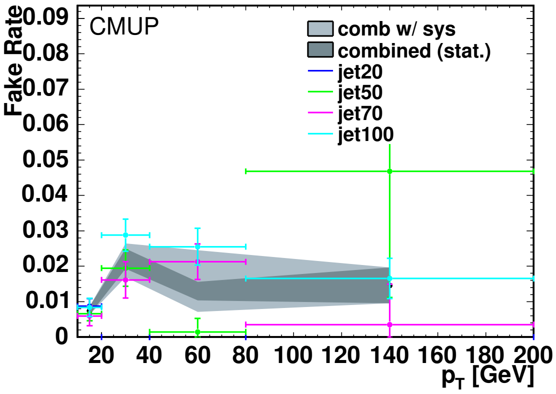

(a) CMUP Fake Rate

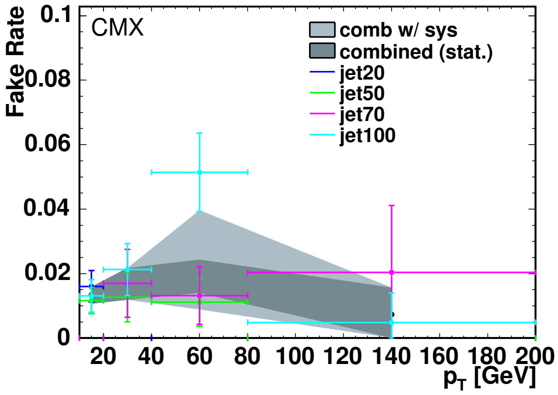

(b) CMX Fake Rate

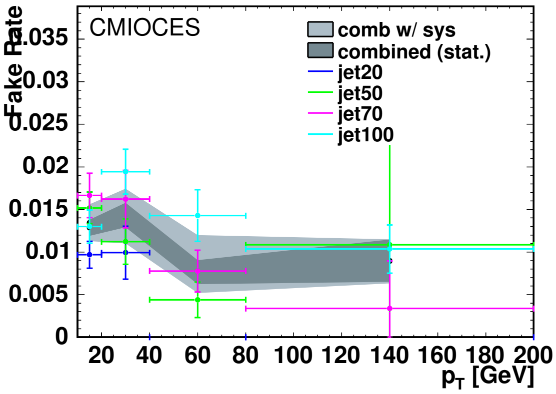

(c) CMIOCES Fake Rate

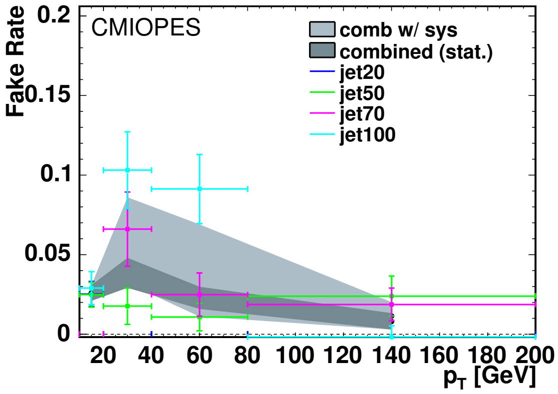

(d) CMIOPES Fake Rate

Figure 7: Jet $\rightarrow$ lepton fake rates for muon types

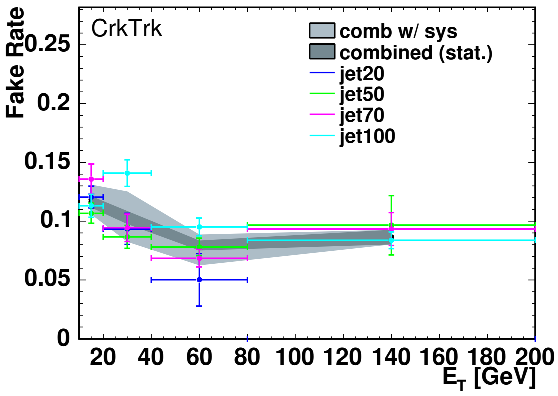

Figure 8: Jet $\rightarrow$ lepton fake rate for CrkTrk type

FakeableCEM (TCE/LCE)
Fiducial Track Fiducial to CES
Had/Em $<= 0.125 + 0.00045E$
Iso/Et $<= 0.3$
IsConversion!=1

FakeablePHX (PHX)
Pes2DEta $1.2 < \|\eta\| < 2$
Had/Em $<= 0.125 + 0.00045E$
PhxMatch True
NSiHits $>= 3$
$\|TrackZ0\| <= 60cm$
Iso/Et $<= 0.3$

FakeablePEM (PEM)
Pes2DEta $1.2 < \|\eta\| < 2.8$
Had/Em $<= 0.125 + 0.00045E$
Iso/Et $<= 0.3$
No PhxMatch with NSiHits$>= 3$ and $\|TrackZ0\| <= 60cm$

Table 12: Selection for central leptons. TCE candidates are the full table and LCE is same as TCE with the cuts in red (in the second box) removed.

FakeableMuonCentral (CMUP/CMX/CMIOCES/CrkTrk)
Track not PES fiducial
NAxL(5 hits) $>= 2$
NStL(5 hits) $>= 2$
Track $\lvert Z_0 \rvert <= 60cm$
Track $\lvert D_0 \rvert <= 0.2cm$ (0.02 cm if NSiHit$>$ 0)
χ^2/dof $<=$ 4 (3 if run $<=$ 186598)
Iso/Et $<= 0.3$

FakeableMuonForward (CMIOPES)
Track PES fiducial
Cot Hit Fraction > 0.6
Track $\lvert Z_0 \rvert <= 60cm$
Track $\lvert D_0 \rvert <= 0.2cm$ (0.02 cm if NSiHit$>$ 0)
χ^2/dof $<=$ 4 (3 if run $<=$ 186598)
Iso/Et $<= 0.3$

Table 13: Selection for central leptons. TCE candidates are the full table and LCE is same as TCE with the cuts in red (in the second box) removed.

Category	Denominators	Z+jets	Z+jets (+1 σ syst)	Z+jets (-1 σ syst)
e e e	9	0.49 $\pm$ 0.16	0.09	-0.09
e e μ	2	0.14 $\pm$ 0.10	0.03	-0.03
e μ μ	0	0.00 $\pm$ 0.00	0.00	0.00
μ μ μ	2	0.06 $\pm$ 0.04	0.03	-0.03
e e trk	2	0.23 $\pm$ 0.16	0.05	-0.05
e μ trk	1	0.01 $\pm$ 0.01	0.00	-0.00
μ μ trk	3	0.11 $\pm$ 0.06	0.03	-0.03
e trk trk	1	0.12 $\pm$ 0.12	0.02	-0.02
μ trk trk	0	0.00 $\pm$ 0.00	0.00	0.00
Total	20	1.14 $\pm$ 0.26	0.26	-0.26

Table 14: Fakes yields in the WZ signal region

running the fake calculation on the Monte Carlo twice. Once as described above requiring that on of the identified leptons is triggerable. The second time we require that neither of the identified leptons in triggerable, and that the fake lepton is triggerable. We then form the ratio of the non-triggerable to triggerable fakes. We find the ratio to be R_{nontrig}=7.0 $\pm$ 1.5%. The total number of fakes is then multiplied by (1+R_{nontrig}) to get the full number of fakes.

The total background from fakes in the WZ analysis using this procedure is estimated to be 1.14 $\pm$ 0.26 before the scaling for nontriggerable fakes, and 1.22 $\pm$ 0.27 after being scaled.

For the ZZ analysis, we predict 0.007$\pm$0.004 events expected from Z+jets based upon the average fake rate in the WZ analysis.

3.4.5 Summary

Table 15 summarizes the expected background yields for the full dataset after selection cuts for ZZ, Zγ, and $t\bar{t}$ physics processes. Table 14 shows the fake background contribution for the WZ search analysis. We expect a total of 2.65$\pm$0.28 background events with a WZ signal expectation of 9.75$\pm$0.03, where errors are statistical only. For ZZ analysis, we expect 1.884$\pm$0.015 signal with 0.007$\pm$0.002 background.

4 Binned Maximum Likelihood Fit

As described in Section 3, we are expecting a close to four standard deviation excess over background in the signal region. In order to maximize our chances of a 5 standard deviation excess, and thus a discovery, we decided to do a Maximum likelihood fit in two bins in MET. We refrain from a full blown unbinned maximum likelihood fit because our

Category	Z+jets	ZZ	$Z\gamma$	$t\bar{t}$	WZ	Total
$e\ e\ e$	0.49	0.09	0.06	0.03	1.98	2.6 $\pm$ 0.2
$e\ e\ \mu$	0.14	0.23	0.00	0.02	1.61	2.0 $\pm$ 0.2
$e\ \mu\ \mu$	0.00	0.06	0.12	0.01	1.28	1.5 $\pm$ 0.1
$\mu\ \mu\ \mu$	0.06	0.15	0.00	0.00	1.02	1.2 $\pm$ 0.1
$e\ e$ trk	0.23	0.11	0.18	0.04	1.39	1.9 $\pm$ 0.2
$e\ \mu$ trk	0.01	0.10	0.04	0.01	1.13	1.3 $\pm$ 0.1
$\mu\ \mu$ trk	0.11	0.10	0.02	0.00	0.83	1.1 $\pm$ 0.1
e trk trk	0.14	0.03	0.01	0.00	0.33	0.5 $\pm$ 0.2
μ trk trk	0.00	0.02	0.00	0.00	0.19	0.2 $\pm$ 0.0
Total	1.21	0.88	0.44	0.12	9.75	12.4 $\pm$ 0.9

Table 15: Expected WZ background yields over the luminosity (signal region)

knowledge of the tails of the MET distribution for background is not sufficient at present to fit this exponentially falling distribution.

Figure 9 shows the MET distributions. The data points shown here are full Geant MC, while the curves are the curves used for the Toy Monte Carlo described below. Fig. 9(c) and 9(d) show properly normalized fits to Drell-Yan and ZZ background respectively. Fig. 9(b) shows the combined background MET distribution. A stacked plot of both of these backgrounds, and the signal is given in Figure 10.

In the present section, we describe the procedure for arriving at the two bins, as well as the expected increase in sensitivity for making a discovery. Section 6 later on in this note describes the fit results, and p-value.

4.1 The Binned Fit

We perform a binned likelihood fit of the MET distribution in two bins using the following likelihood function:

$$\begin{array}{ccc}
\mathcal{L}(N_s) & = & \frac{\mu_1^{N_1} e^{-\mu_1}}{N_1!} \times \frac{\mu_2^{N_2} e^{-\mu_2}}{N_2!} \\
\mu_i & = & N_s \times \epsilon_i^s + N_{bkg}^{expected} \times \epsilon_i^{bkg} \\
N_i & = & \text{observed yield in bin i} \\
1 & := & \epsilon_1^s + \epsilon_2^s \\
N_{bkg}^{expected} & = & \text{predicted \# of background events}
\end{array} \quad (3)$$

Note that $N_{bkg}^{expected}$ is the mean expected background summed over both bins. It is a fixed number, predicted from Monte Carlo studies plus fake rates as described in Section 3. This likelihood function in one variable, N_s, can be maximized analytically.

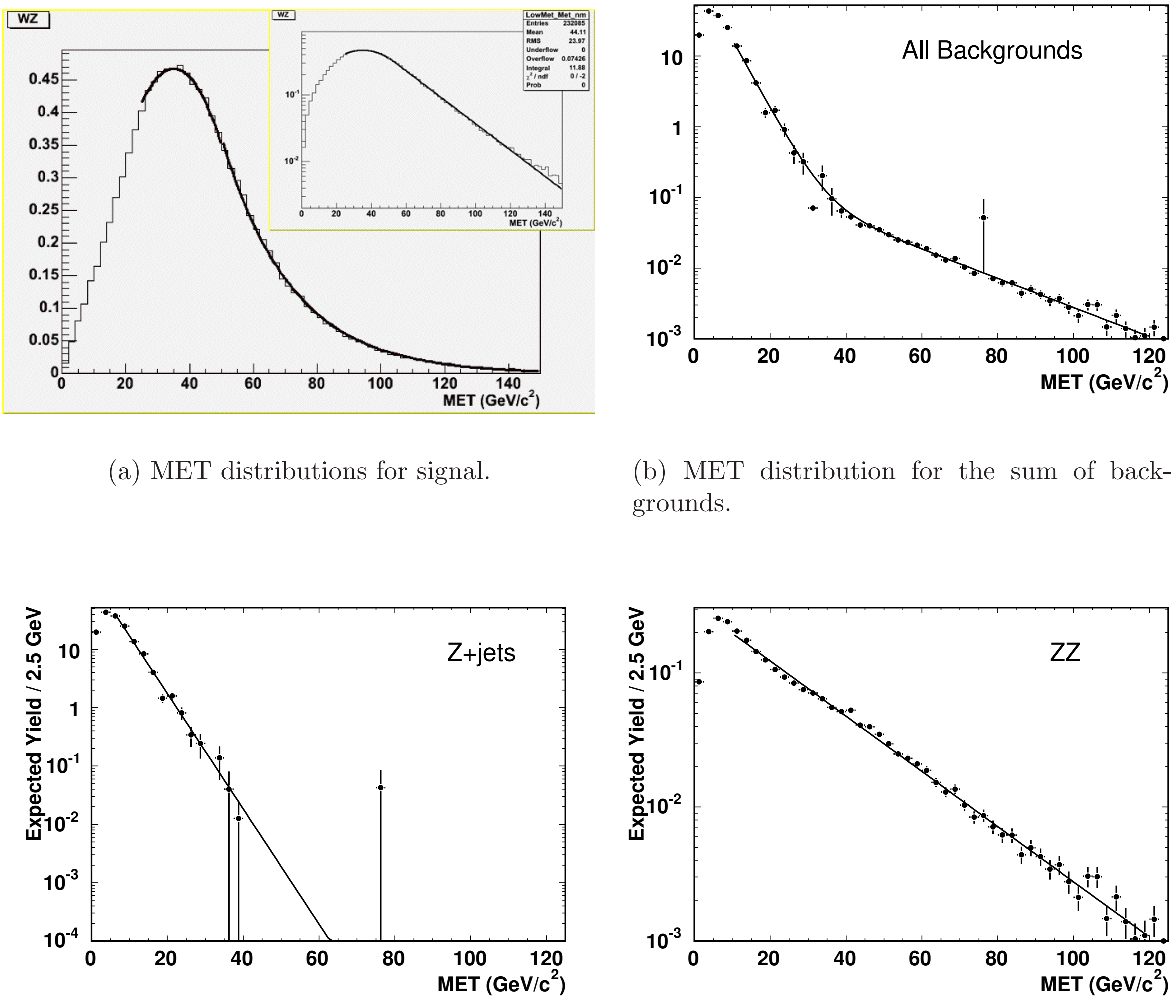

(a) MET distributions for signal.

(b) MET distribution for the sum of backgrounds.

(c) MET distributions for Drell-Yan background.

(d) MET distribution for ZZ background.

Figure 9: MET distributions for signal and background MC, and the fits used in the TOY MC.

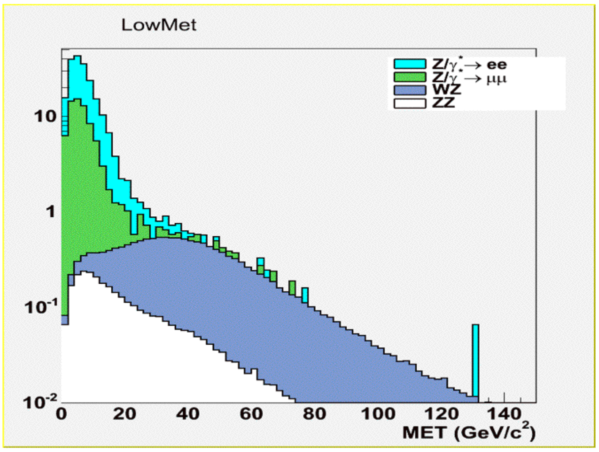

Figure 10: MET distributions for signal, background MC in ZZ and Drell-Yan.

For this likelihood fit we record the likelihood ratio, λ_x, defined as:

$$\lambda_x = -2log\mathcal{L}(best\ fit) + 2log\mathcal{L}(zero\ signal) \quad (4)$$

The subscript "x" here is meant to indicate the binning chosen.

4.2 Optimizing the binning

We do the fit described above for a large number of toy experiments, each of which consists of MET values for a Poisson fluctuating number of signal and/or background events, drawn from the expected MET distributions. As the expected number of background events itself has some uncertainty, we chose to draw the mean for the background Poisson distribution from a Gaussian that reflects the error on the expected background. At the same time, the likelihood function used to fit for N_s uses the nominal 2.24 expected background events throughout.

Following a suggestion by Giovanni Punzi, we determine the optimal binning as follows:

1. Generate toy experiments with background only. Determine λ_x^{bkg} for each of these toy experiments. Determine the λ_x^{cut} for which no more than 5.7×10^{-7} (i.e. 5σ one sided tail) of experiments have $\lambda_x^{bkg} > \lambda_x^{cut}$.

2. Now generate experiments including signal and background events according to the Poisson fluctuations around the expected yields. Determine the fraction of λ_x^{s+bkg} above λ_x^{cut}. This is called the "power" of the binning x.

3. Repeat the procedure for all binnings x, and find the binning with the largst "power". I.e. for which the fraction of $\lambda_x^{s+bkg} > \lambda_x^{cut}$ is largest.

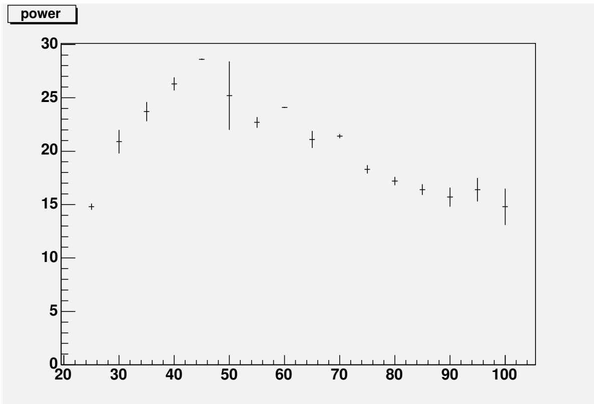

Figure 11: “Power” of a binning as a function of bin boundary.

We chose values for “x” from 30GeV to 100GeV in increments of 5GeV, and generated for each binning 50 Million experiments. The statistics defining the 5σ tail is thus 28.5 experiments, sufficiently large to get a reasonable measurement of λ_x^{cut}. Fig. 11 shows the resulting “power” as a function of the binning. As a reference, we also added a toy experiment without any binning. Here N_s is simply the yield in the signal region minus the expected background. In this case N_s itself is used instead of λ_x as no fit is performed.

The errors on each point were estimated as follows. There is roughly a 20% error due to Poisson statistics of the 28.5 experiments in the 5σ tail. This translates into an uncertainty of λ_x^{cut}. In addition, the set of possible values for N_s as well as λ_x^{cut} are discreet rather than continuous. We thus find the two discreet values that bracket the desired λ_x^{cut}, and use the slopes of the λ_x distribution for background only and signal & background distributions to calculate the error on the power due to the error on λ_x^{cut}.

We conclude that a two bin likelihood fit with a bin boundary at 45GeV roughly doubles our chances of measuring a signal yield with statistical significance of 5σ or more.

4.3 Expected Results

Fig. 12(a) shows the distribution of expected λ_{45} for background only, and signal & background. Once we “open the signal box” and fit for N_s we will use the background only distributions to determine the p-value. Fig. 12(b) shows the $-2log\mathcal{L}$ distribution for an example outcome that we might find. Here, $N_1 = 6$ and $N_2 = 5$ events respectively. This particular example has a p-value of about 2×10^{-5}. We note that the likelihood function does not take the uncertainty on the background expectation into account, while the p-value does.

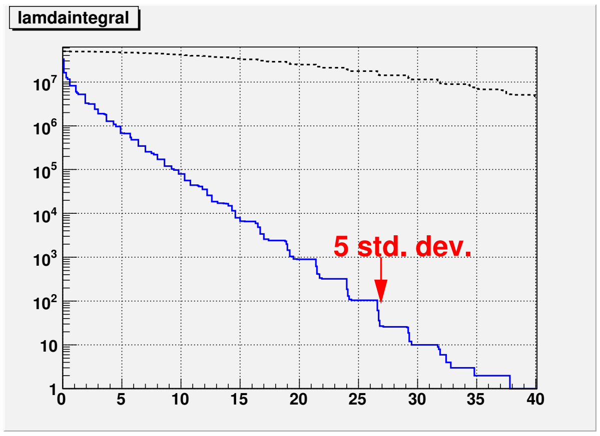

(a) Integral of λ_{45} for Toy Monte Carlo including background only (black) and signal & background (blue).

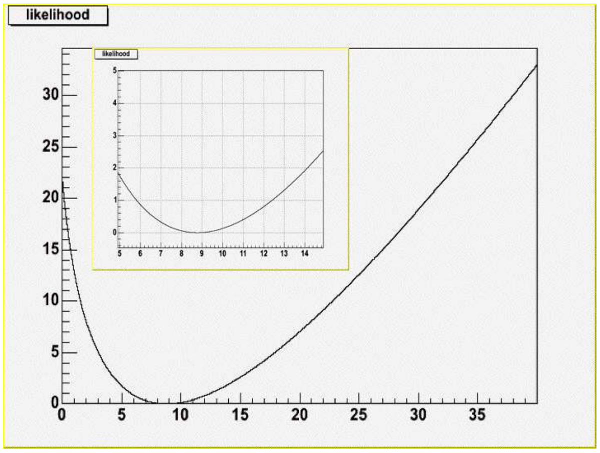

(b) Example $-2log\mathcal{L}$ curve for nominal yields.

5 Cross checks

In this section, we present the cross checks we have performed. These include comparisons of expected an observed events in regions which exclude the signal region for our WZ search analysis. Analysis of these regions test our determination and application of lepton ID scale factors, fake rates, trigger efficiencies, and good run / luminosity accounting. The control regions we consider are:

- Dilepton, Z Mass Region (Drell-Yan)
- Trilepton, Low $\not\!\!E_T$, Z Mass Region
- Trilepton, Low $\not\!\!E_T$, no-Z Mass Region

There are no four lepton control regions we consider.

In the trilepton regions, we double-check that our fake and conversion is sensible by also doing to the comparison using Pythia DY MC without HEPG matching. This means that we now have jet fake contributions from the MC which can be used as a cross check in the high statistics control regions.

5.1 Dilepton Z Mass Region (Drell-Yan)

Here we consider opposite-sign same-flavor dileptons in the Z mass region which is completely dominated by the Drell-Yan process. We require one trigger leg and the other leg has $E_T > 10$ GeV. We also require $\not\!\!E_T < 20$ GeV in this region.

Table 16 and Figure 12 show the agreement between the expected number of events and the observed yield for each dilepton catagory and also these combined into ee and $\mu\mu$. Figures 13 and 14 show some kinematic distributions normalized to the expected number of events from Monte Carlo for the full dataset for ee and $\mu\mu$, respectively. We generally find good agreement in the shapes and normalizaton.

Appendix A shows the kinematic plots separately for each of the dilepton categories.

Category	$Z \to ee$ MC	Data	Data/MC
TCE TCE	22564	22329	1.011 $\pm$ 0.007
TCE LCE	2006	2071	0.968 $\pm$ 0.022
TCE PHX	21829	22143	0.986 $\pm$ 0.007
TCE PEM	11900	10988	1.083 $\pm$ 0.010
TCE Trk	11009	11084	0.993 $\pm$ 0.009
e e	57450.37$\pm$56.73	58299	1.015 $\pm$ 0.001
e trk	11166.56$\pm$24.96	11009	0.986 $\pm$ 0.002
Total $Z \to ee$	68616.93$\pm$61.98	69415	1.012 $\pm$ 0.001

Category	$Z \to \mu\mu$ MC	Data	Data/MC
CMUP CMUP	5255	5202	0.990 $\pm$ 0.014
CMUP CMX	4852	4890	1.008 $\pm$ 0.014
CMX CMX	1361	1351	0.992 $\pm$ 0.027
CMUP CMIOCES	8438	8931	1.058 $\pm$ 0.011
CMX CMIOCES	3956	4125	1.042 $\pm$ 0.016
CMUP CMIOPES	6230	5999	0.963 $\pm$ 0.012
CMX CMIOPES	2945	2796	0.949 $\pm$ 0.018
CMUP Trk	7445	7337	0.985 $\pm$ 0.012
CMX Trk	3603	3545	0.984 $\pm$ 0.017
μ μ	33041.41$\pm$43.81	33294	1.008 $\pm$ 0.001
μ trk	11048.92$\pm$25.28	10882	0.985 $\pm$ 0.002
Total $Z \to \mu\mu$	44092.97$\pm$50.59	44182	1.002 $\pm$ 0.001

Table 16: Predicted and observed Z yields.

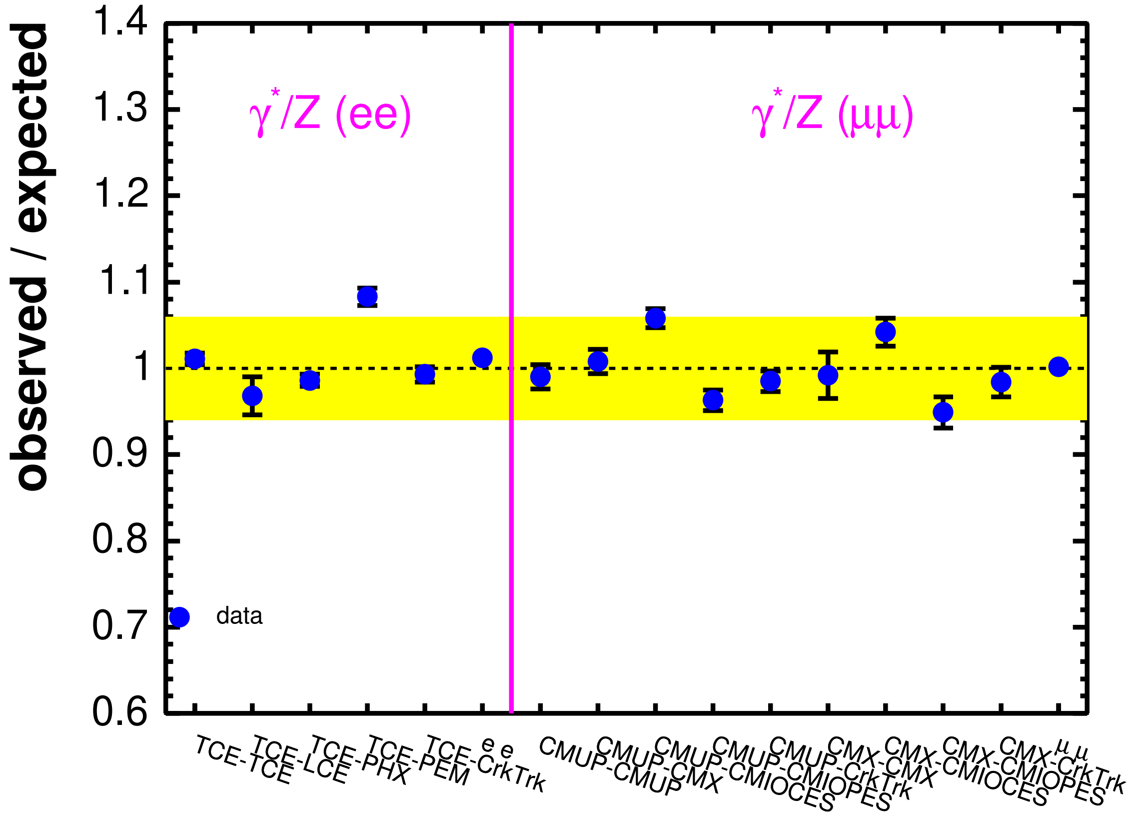

Figure 12: Comparison of expected and observed events in the dilepton control region.

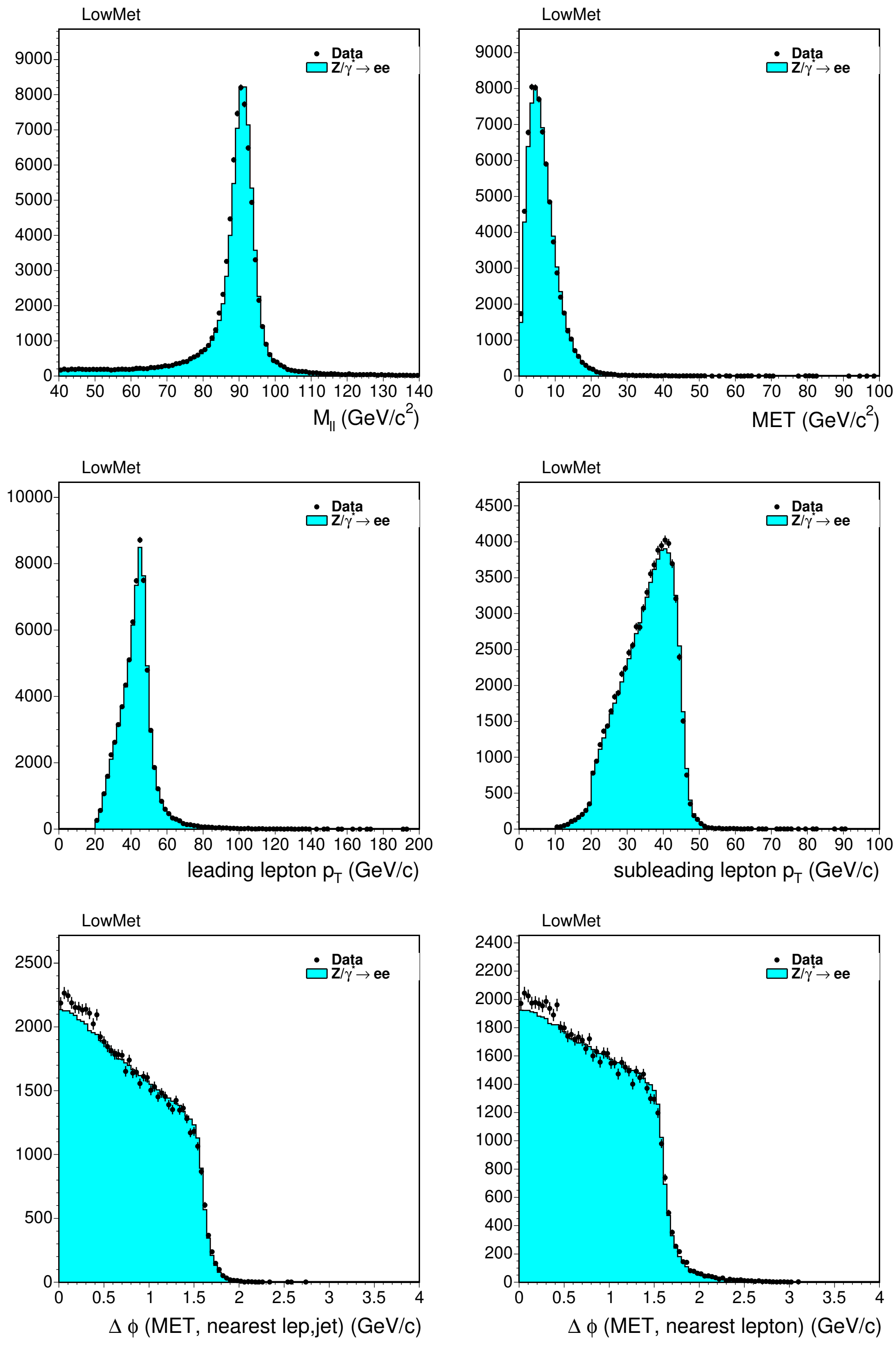

Figure 13: Drell-Yan ($Z \to e^+e^-$) control region.

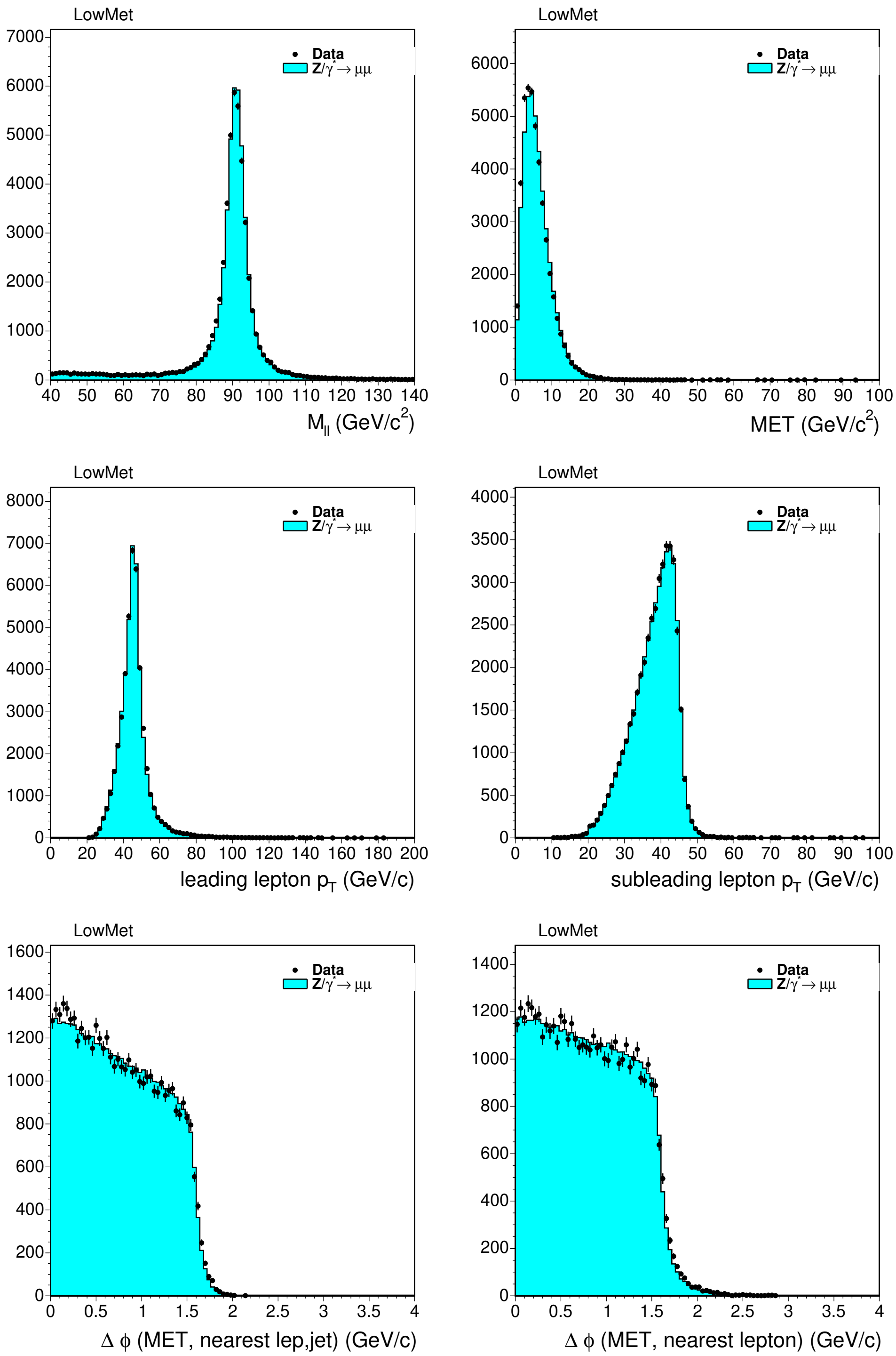

Figure 14: Drell-Yan ($Z \rightarrow \mu^+\mu^-$) control region.

Category	Z+jets	ZZ	$Z\gamma$	$t\bar{t}$	WZ	Total	Data
e e e	29.71	0.55	85.45	0.01	0.59	116.3 ± 19.2	103
e e μ	1.01	0.28	0.01	0.01	0.46	1.8 ± 0.3	2
e μ μ	15.59	0.38	46.11	0.00	0.40	62.5 ± 10.3	50
μ μ μ	0.67	0.19	0.00	0.00	0.28	1.1 ± 0.2	1
e e trk	8.92	0.33	19.92	0.00	0.41	29.6 ± 4.6	20
e μ trk	5.94	0.27	18.39	0.00	0.33	24.9 ± 4.1	33
μ μ trk	1.83	0.17	0.52	0.00	0.23	2.7 ± 0.4	5
e trk trk	1.66	0.07	2.19	0.00	0.10	4.0 ± 0.7	1
μ trk trk	0.14	0.04	0.17	0.00	0.05	0.4 ± 0.2	0
Total	65.59	2.28	172.75	0.02	2.84	243.5 ± 38.8	215

Table 17: Expected yields over the luminosity (low $\not\!\!E_T$ region)

5.2 Trilepton Z Mass, Low $\not\!\!E_T$ Region

In this section, we show the trilepton data compared to our background expectations after full selection except the $\not\!\!E_T$ cut which is reversed to be < 25 GeV. This region is dominated by ISR $Z\gamma$ and Z+jet fakes and therefore provides a test of our background determination outside of our signal region.

Table 17 shows the comparisons between expected and observed events.

5.3 Trilepton Z-veto, Low $\not\!\!E_T$ Region

In this control region, we invert both the $\not\!\!E_T$ and Z-mass cut as compared to the signal region. This region is dominated by $Z\gamma$ FSR.

Table 18 shows the comparisons between expected and observed events.

5.4 Control region summary

The dilepton and both trilepton low $\not\!\!E_T$ control regions agree well with our predictions. In Figure 5.4, we show this graphical. The Pythia Drell-Yan model also agrees remarkably well with the data and our model.

5.5 Fake rate calculation cross-check

As a cross-check, we propagated the fake rates that correspond to different leading jet cuts in the fake rate calculation as described in CDF Note 8538 [8]. The variations, shown in Figure 5.5, are small and consistent with the assigned systematic uncertainties.

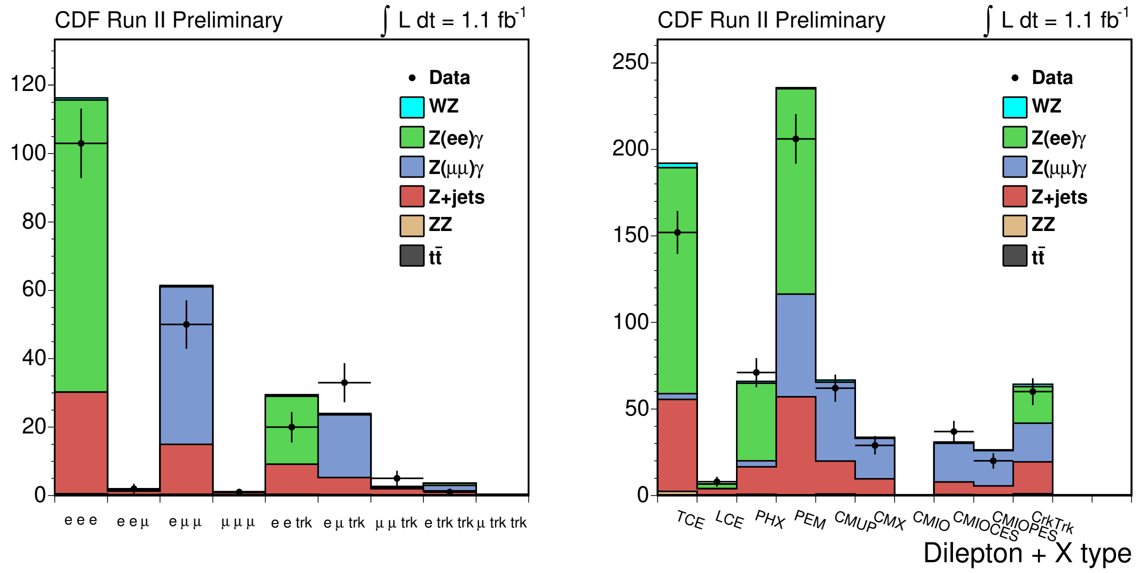

Figure 15: Trlepton Z mass, Low $\not\!\!E_T$ control region.

Category	Z+jets	ZZ	$Z\gamma$	$t\bar{t}$	WZ	Total	Data
$e\ e\ e$	11.16	0.12	103.39	0.01	0.09	114.8 $\pm$ 22.5	103
$e\ e\ \mu$	1.29	0.06	0.01	0.01	0.07	1.4 $\pm$ 0.4	4
$e\ \mu\ \mu$	3.17	0.07	65.92	0.01	0.05	69.2 $\pm$ 14.0	62
$\mu\ \mu\ \mu$	0.28	0.02	0.00	0.00	0.02	0.3 $\pm$ 0.1	1
$e\ e$ trk	4.58	0.07	28.76	0.00	0.08	33.5 $\pm$ 6.2	31
$e\ \mu$ trk	2.08	0.06	24.32	0.00	0.07	26.5 $\pm$ 5.2	34
$\mu\ \mu$ trk	0.88	0.02	0.98	0.00	0.02	1.9 $\pm$ 0.4	3
e trk trk	0.13	0.02	2.38	0.00	0.02	2.6 $\pm$ 0.5	2
μ trk trk	0.13	0.01	0.27	0.00	0.01	0.4 $\pm$ 0.1	1
Total	23.93	0.44	226.03	0.03	0.44	250.9 $\pm$ 48.3	241

Table 18: Expected yields over the luminosity (Z-veto, low $\not\!\!E_T$ region)

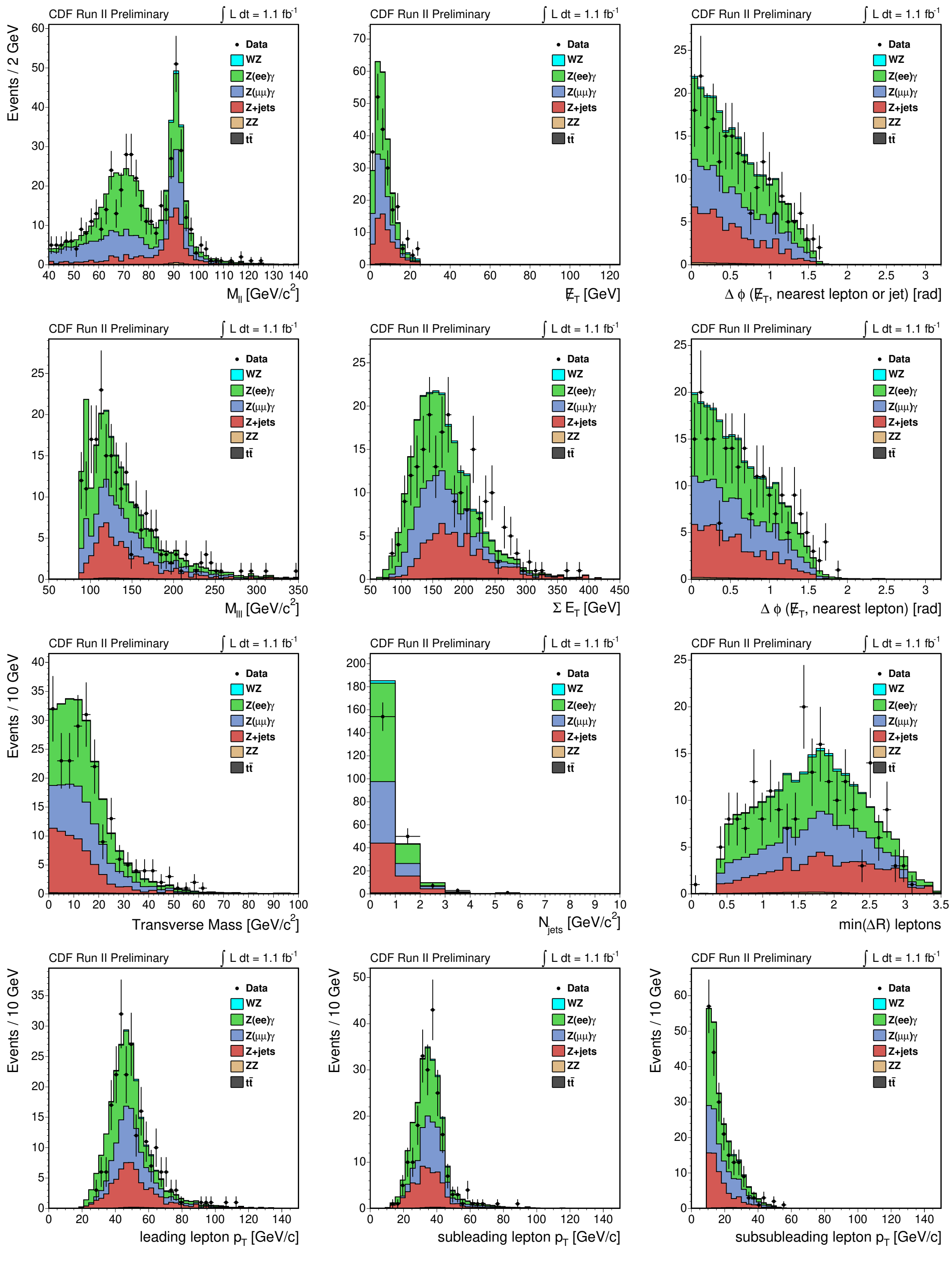

Figure 16: Trlepton Z mass, Low $\not\!\!E_T$ control region.

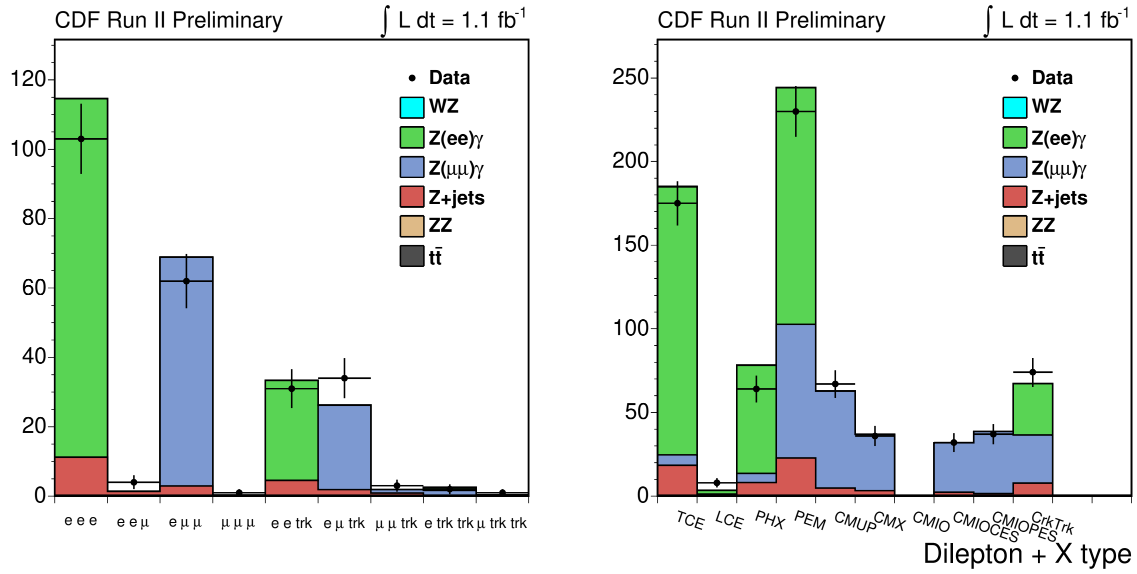

Figure 17: Trilepton Z-veto mass, Low $\not\!\!E_T$ control region.

6 Observed Yield

In the signal region for the WZ analysis, we observe 16 candidate events. Table 15 summarizes the expected background yields for the full dataset after selection cuts for ZZ, Zγ, and $t\bar{t}$ physics processes along with the observed numbero of events for each trilepton type.

The trilepton types in the signal region are summarized in Figure 21. The kinematic distributions in the signal region are shown in Figure 22. The $\not\!\!E_T$ distribution (linear and log scale) for the full range is shown in Figure 23.

6.1 Statistical Analysis of the Yield

As discussed in Section 4, we decided to perform a binned maximum likelihood fit prior to opening the signal box in order to use the information in the MET shape in addition to the number of events in the signal box. This was thought necessary to maximize the chances of arriving at a 5σ statistically significant result.

We find that 7 of the 16 events in the signal box have $MET > 45$GeV. Figure 24 shows the likelihood curve for the binned fit with $N_1 = 9; N_2 = 7$ as yields for the two bins. The difference in $-2log\mathcal{L}$ between best fit and the zero signal hypothesis is 37.75. We refer to this likelihood ratio as λ. Interpreting this as a χ^2 would signify a signal with more than 6σ statistical significance.

We now ask ourselves the following three statistical questions:

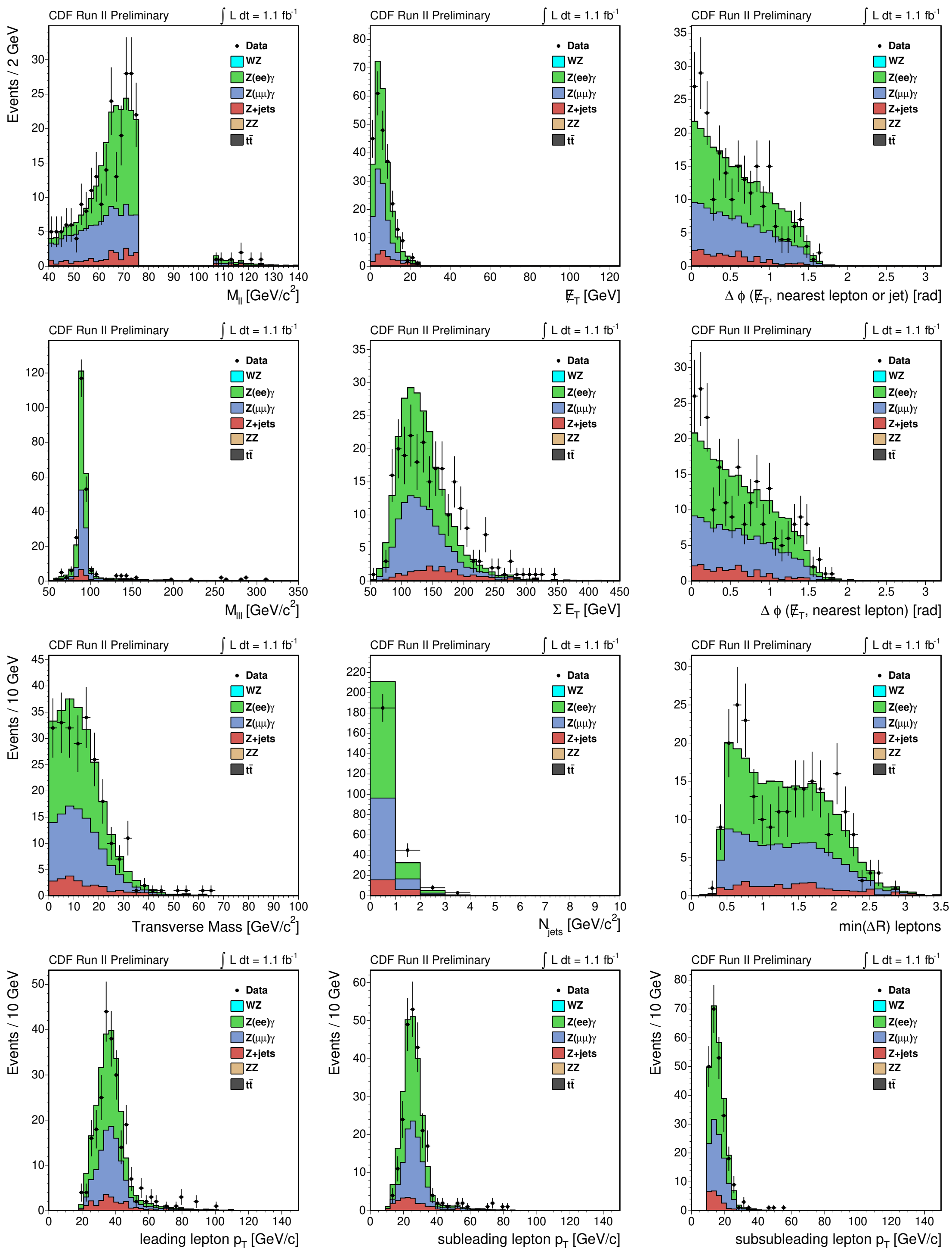

Figure 18: Trilepton Z-veto mass, Low $\not\!\!E_T$ control region.

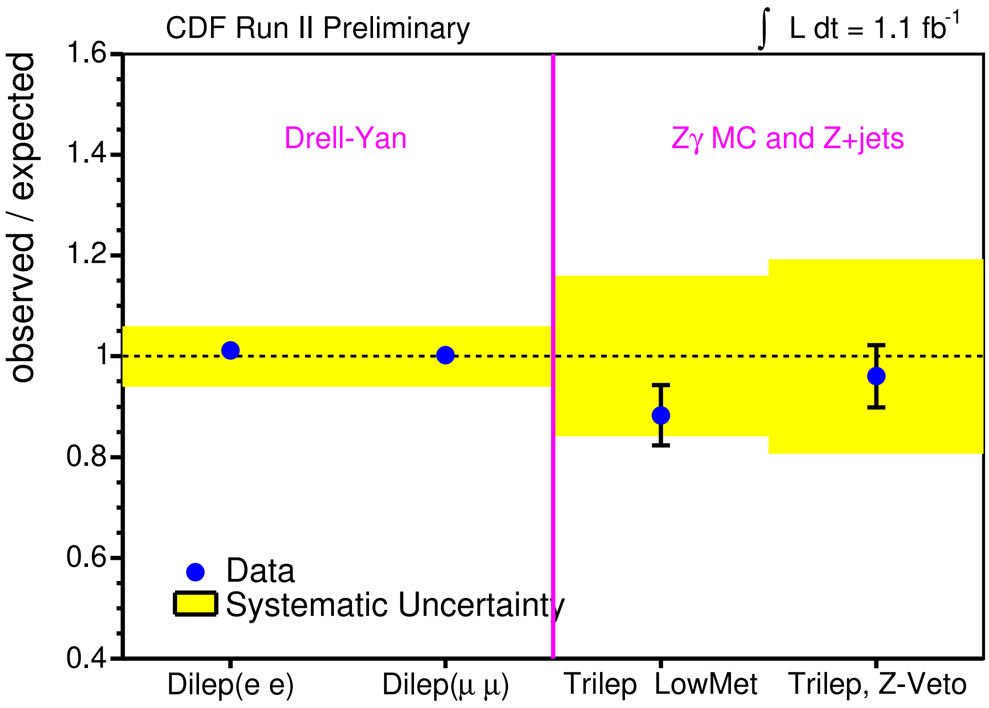

Figure 19: Summary of the control region results

Category	Z+jets	ZZ	$Z\gamma$	$t\bar{t}$	WZ	Total	Data
$e\ e\ e$	0.49	0.09	0.06	0.03	1.98	2.6 ± 0.2	6
$e\ e\ \mu$	0.14	0.23	0.00	0.02	1.61	2.0 ± 0.2	0
$e\ \mu\ \mu$	0.00	0.06	0.12	0.01	1.28	1.5 ± 0.1	1
$\mu\ \mu\ \mu$	0.06	0.15	0.00	0.00	1.02	1.2 ± 0.1	1
$e\ e$ trk	0.23	0.11	0.18	0.04	1.39	1.9 ± 0.2	5
$e\ \mu$ trk	0.01	0.10	0.04	0.01	1.13	1.3 ± 0.1	2
$\mu\ \mu$ trk	0.11	0.10	0.02	0.00	0.83	1.1 ± 0.1	1
e trk trk	0.14	0.03	0.01	0.00	0.33	0.5 ± 0.2	0
μ trk trk	0.00	0.02	0.00	0.00	0.19	0.2 ± 0.0	0
Total	1.21	0.88	0.44	0.12	9.75	12.4 ± 0.9	16

Table 19: Expected WZ background yields over the luminosity (signal region) and the observed number of events

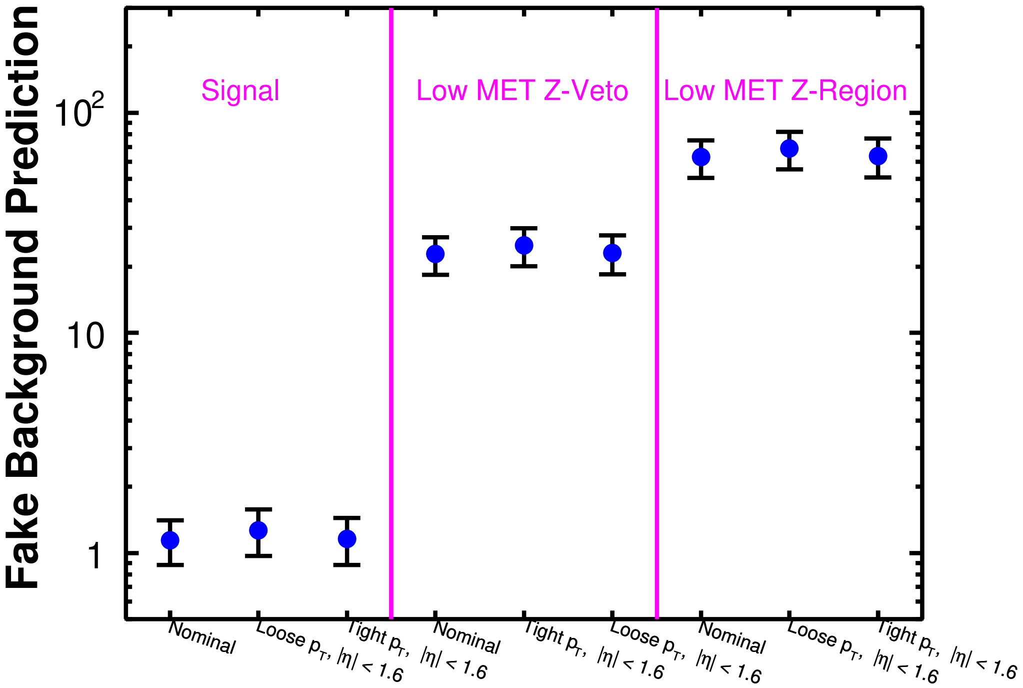

Figure 20: Variations in the predicted Z+jets background in the Signal and Control Regions

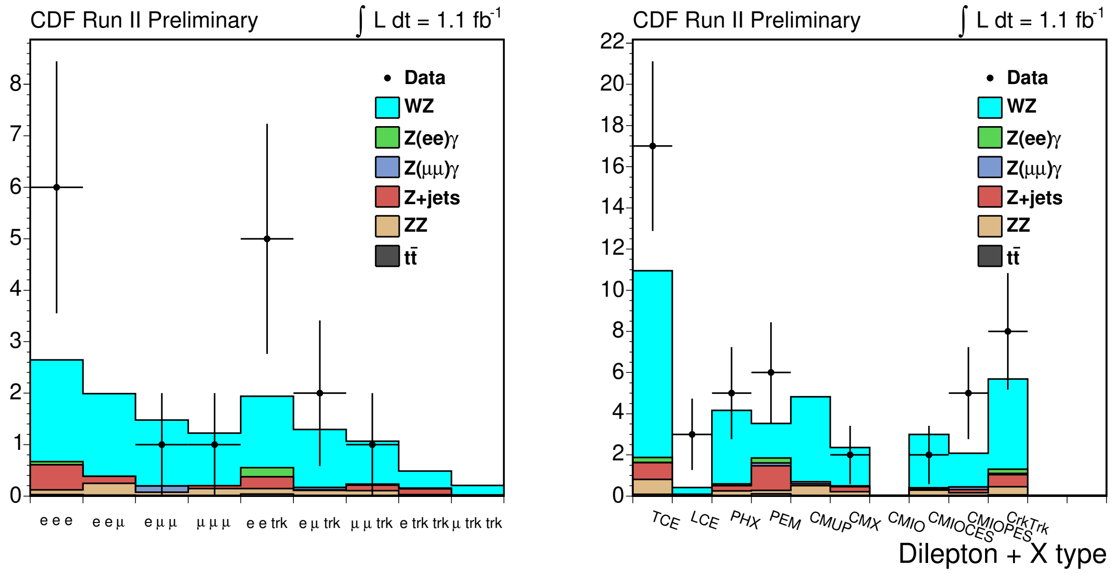

Figure 21: WZ signal region.

- What's the probability for an expected background yield to fluctuate to the observed 16 events, or more? We evaluate this by drawing a number of events from a Poison distribution with a mean that is drawn from a Gausian distribution according to the expected background and its error. We throw backgrounds from physics (1.01 ± 0.108) seperately from background due to fakes (1.70 ± 0.42) to be consistent with our MET fitting significance test described below. We repeat this procedure 500 Million times, and find that in 73/500 Million we get a value of 16 or higher. We thus estimate the probability for background to fluctuate to the 16 events signal we observe as $\sim 1.46 \times 10^{-7}$. For comparison, the probability of picking a number from the 5σ one sided tail of a Gausian distribution is 2.85×10^{-7}. We thus conclude that our statistical significance is 5.1σ even for the yield alone, i.e. ignoring the MET distribution of the events in the signal region.

- What's the probability for an expected background yield of 1.70 ± 0.42 events with a MET distribution like Drell-Yan, and 1.01 ± 0.108 events with a MET distribution like ZZ, to lead to a binned fit with $\lambda \geq 37.75$? To answer this question, we draw 1 Billion Toy experiments, each of which includes only background events. We draw the number of events for each background hypothesis from a Poison distribution who's mean is drawn from a Gaussian according to the expected background. We then draw MET values from the MET distributions for the two background hypotheses. For each experiment, we then perform the two bin likelihood fit, and calculate λ. We find that two of the 1 Billion toy Monte Carlo experiments leads

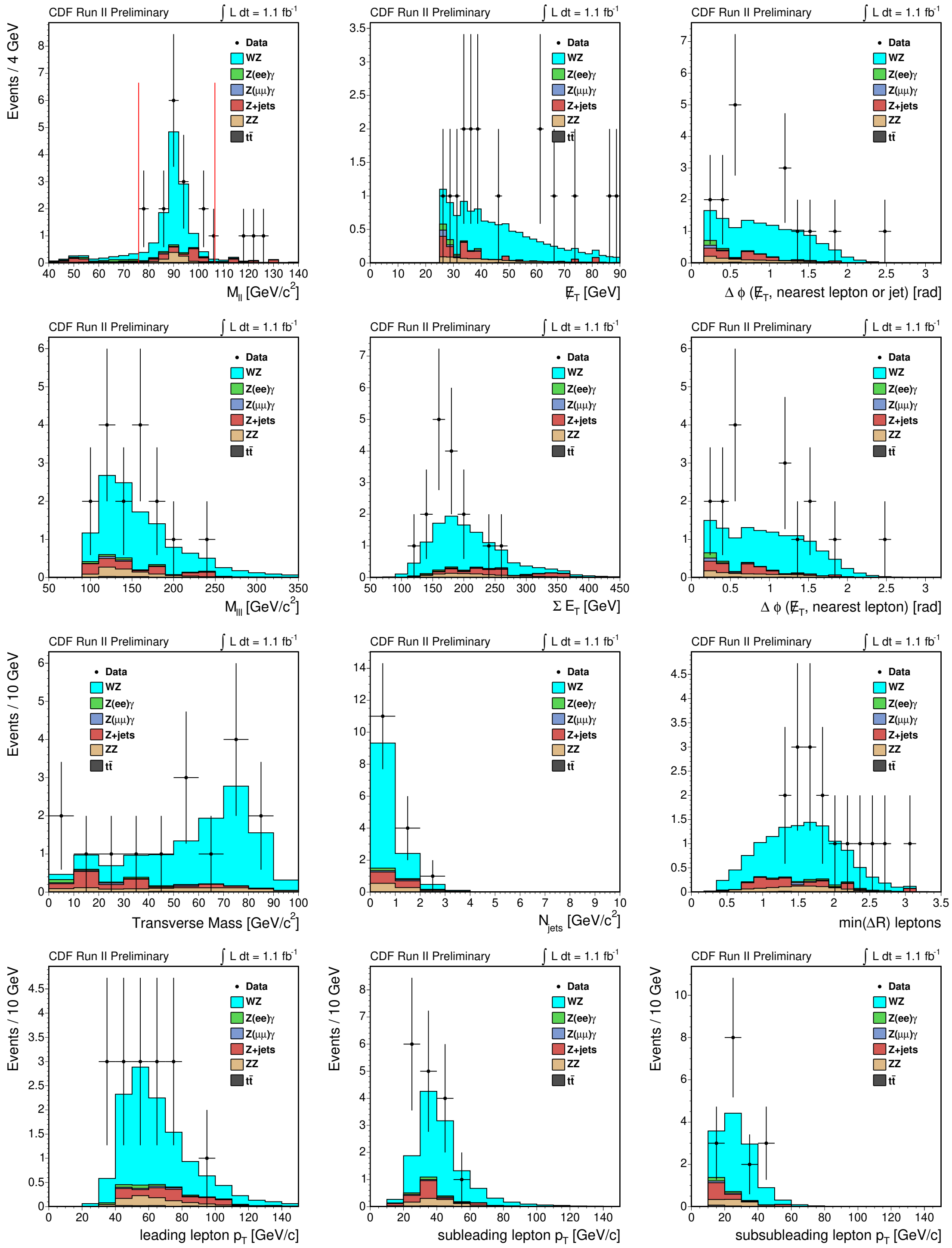

Figure 22: WZ signal region

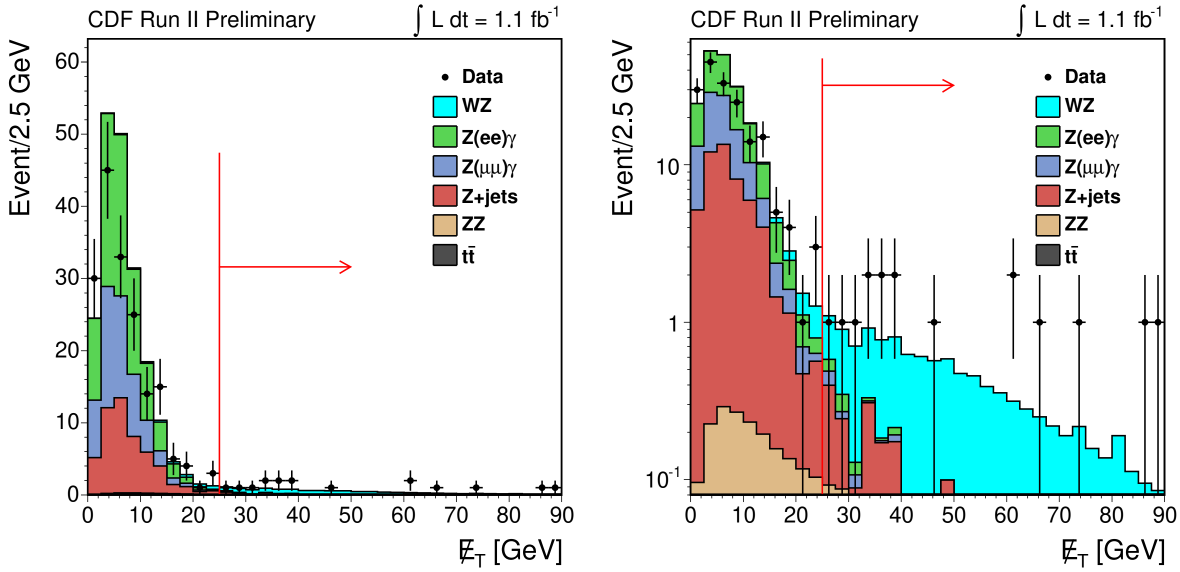

Figure 23: Full $\not{E}_T$ region for WZ analysis

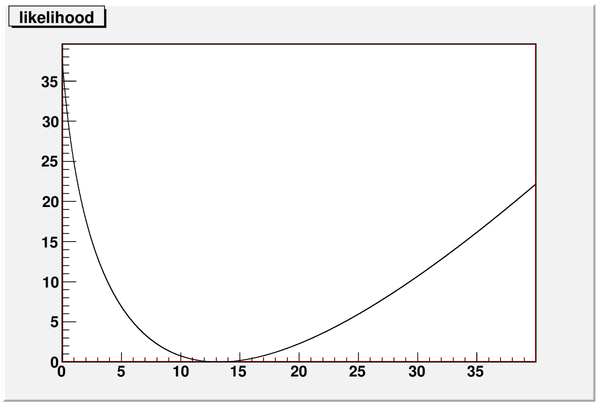

Figure 24: Binned Maximum Likelihood Fit Result.

to a $\lambda \geq 37.75$. For comparison, the probability to draw a number from a Gaussian distribution and have it fall into the one sided 6σ tail is 1/Billion. We thus conclude that our significance overall is 5.9σ.

- Finally, we ask ourselves to what extend our yield and MET distribution is expected given the expected number of signal and background events. We evaluate this by computing the product of the Poison probabilities for the yields $N_1 = 9; N_2 = 7$, and comparing it with expectations for Toy Monte Carlo experiments drawn from the nominal distributions. We find that 4,887 out of 10,000 experiments have a product of Poison probabilities smaller than our data.

Based on this statistical analysis, we conclude that we have observed a yield in our WZ search that has a statistical significance of 5.9σ even after taking into account the uncertainty on the background expectations. Moreover, the yield observed, both in terms of total number of events as well as MET distribution across our two MET regions, is perfectly consistent with Standard Model WZ production plus the known backgrounds.

7 Systematics

In this section we assess the systematics on our WZ and ZZ cross section determination.

7.1 Signal and Background acceptance

7.1.1 Jet Energy Scale

Since we do not make an explicit cut on jet multiplicity but rather jets are used only to correct the $\not{E}_T$, we do not assign a systematic due to jet energy scale.

7.1.2 Lepton ID Scale Factors

The effect of the lepton ID scale factors is determined by propagating the scale factor uncertainties through the analysis. The effects are 1-2%, detailed numbers are shown in Tables 20 and 21.

7.1.3 Trigger efficiency

The effect of the trigger efficiencies uncertainies also propagated through the analysis. The results are $\approx 0.2\%$. In the trigger efficiency calculation, we assume that the LCE category does not cause triggers. To assess a systematic on this assumption count the LCE category as triggerable, which results in shifts of order 0.5%. Finally, we consider the possibility that electrons with $\mathrm{p_t}$ less than 20 GeV can cause a trigger by lowering the $\mathrm{p_t}$ threshold to consider a candidate triggerable to 18 GeV. This result in a neglible shift. The total trigger efficiency systematic the result of adding these three studies in quadrature.

7.1.4 PDF Systematics

The sensitivity of the acceptance to the choice of PDF has been studied for WW in [11] and also WZ, ZZ in [6]. In both cases, they arrive at 2% systemtic uncertainty on the acceptance due to PDF shape, which is the uncertainty we quote for both WZ and ZZ.

7.1.5 Energy Scale/Resolution

In the previous CDF Note 8095 [3], the energy scale and resolutions were found to be neglibly small effects because the cut on invariant mass of (76, 106) GeV is loose. We use the same conservative 1% uncertainty on the signal and background acceptances for Z+X.

7.1.6 $\not\!\!E_T$ Modeling

The $\not\!\!E_T$ modeling systematic uncertainty the WW signal acceptance was determined in CDF 8094[11] using a re-weighting technique to be very small: 0.3%. Although the $\not\!\!E_T$ distributions are slightly different for WW and WZ, the $\not\!\!E_T$ calculation for both analyses is identical and so we assign a conservative systematic uncertainty of 1.0% on the WZ acceptance.

The $\not\!\!E_T$ distribution of the ZZ as a background to WZ is determined primarily by lost muons and therefore has very similar uncertainties to the WW and WZ, so we assign a 1.0% uncertainty on the ZZ as a backgroun to WZ.

7.1.7 Fake Background

We estimate the uncertainties on the fake background by varying the fake rates within their assigned uncertainties (shown by the solid band in Figures 6 through 3.4.4, which arises from the difference between the different jet samples.) Using this procedure, we assign a systematic uncertainty of 25% for WZ and ZZ fake background.

7.1.8 Conversion Scale Factor for Zγ

The $Z\gamma$ mode enters the WZ selection when the photon is reconstructed as an electron and we also have large $\not\!\!E_T$. This is usually due to a conversion. In the TCE selection, we explicitly veto conversions, but the efficiency of this veto may not be well modeled in the Monte Carlo.

For the PEM electron category, there is no suppresion of photons. This means that the main descrimination against $Z\gamma$ is the $\not\!\!E_T$ requirement. In order to limit how well the $\not\!\!E_T$ distribution is modeled in the Monte Carlo, we use the estimate from the WW measurement of 25% [3].

Based upon the studies in CDF Note 8073[9] Attal et al. on the conversion modeling, and combining the conversion scale factor, material uncertainty, and normalization uncertainty, we apply a 20% systematic uncertainty on the Zγ background. This uncertainty dominates other uncertanties such a k-factor uncertainties for the difference between LO and NLO cross-sections.

We combine the $\not\!\!E_T$ and conversion uncertainties we get a 32% uncertainty on the $Z\gamma$ background to WZ.

7.1.9 ZZ and $t\bar{t}$ Cross Sections for Backgrounds

Both ZZ and $t\bar{t}$ can produce background in the WZ channel. The dominant uncertainties for both of these is the cross-section. We add the cross-section uncertainties described below with the trigger, lepton id, and $\not\!\!E_T$ modeling systematics described above.

For the ZZ cross-section uncertainty, we take the half the difference between LO and NLO cross section as an estimate of the effect of higher or calculation. This is 10% ZZ cross section, which we assign as a systematic uncertainty.

For $t\bar{t}$ we use the standard quote uncertainty on the NLO cross-section, 6.7 ± 0.7 *pb*, which is also 10%.

7.2 Summary

A summary of the systematic uncertainties is shown in Table 20 for the WZ acceptance and backgrounds and Table 21 for ZZ acceptance.

Our total expected yield for WZ in trileptons, not including cross-section or luminosity errors, is

$$9.75 \pm 0.03(stat.) \pm 0.31(syst.)$$

The expected background yields are:

Z+jets	1.21 ± 0.27 (stat.) ± 0.28 (syst.) ± 0.00 (lumi.)
ZZ	0.88 ± 0.01 (stat.) ± 0.09 (syst.) ± 0.05 (lumi.)
$Z\gamma$	0.44 ± 0.05 (stat.) ± 0.14 (syst.) ± 0.03 (lumi.)
$t\bar{t}$	0.12 ± 0.01 (stat.) ± 0.01 (syst.) ± 0.01 (lumi.)

The total background expectation is

$$2.65 \pm 0.28(stat.) \pm 0.33(syst.) \pm 0.09(lumi.)$$

Our total expected yield for ZZ in four leptons, not including luminosity errors, is

$$1.884 \pm 0.015 \pm 0.064$$

The expected background yields are:

Variation	ZZ	$Z\gamma$	$t\bar{t}$	WZ
Nominal	0.886	0.479	0.121	9.794
LepId $\pm 1\sigma$	$\pm$ 2.0 %	$\pm$ 1.9 %	$\pm$ 1.2 %	$\pm$ 1.9 %
TrigEff $\pm 1\sigma$	$\pm$ 0.2 %	$\pm$ 0.3 %	$\pm$ 0.4 %	$\pm$ 0.2 %
Trigger on LCE	0.6 %	0.8 %	0.0 %	0.5 %
Trigger turn on	0.0 %	0.0 %	0.0 %	0.0 %
Total TrigEff	$\pm$ 0.6 %	$\pm$ 0.9 %	$\pm$ 0.4 %	$\pm$ 0.6 %
$\not\!\!E_T$ Modeling	$\pm$ 1.0%	$\pm$ 25.0%	$\pm$ 1.0%	$\pm$ 1.0%
Energy Scale	$\pm$ 1.0%	$\pm$ 1.0%	-	$\pm$ 1.0%
PDF Uncertainty	$\pm$ 2.0%	$\pm$ 2.0%	$\pm$ 2.0%	$\pm$ 2.0%
Cross-section	$\pm$ 10.0%	$\pm$ 20.0%	$\pm$ 10.0%	-
Total	10.5 %	32.2 %	10.3 %	3.2 %

* include conversion and material description systematics.

Table 20: Summary of the systematic uncertainties on the WZ acceptance and Monte Carlo derived backgrounds

Source	Uncertainty
Nominal	1.884
LepId $\pm 1\sigma$	$\pm$ 2.2 %
TrigEff $\pm 1\sigma$	$\pm$ 0.2 %
Trigger on LCE	0.8 %
Trigger turn on	0.1 %
Total TrigEff	$\pm$ 0.8 %
$\not\!\!E_T$ Modeling	$\pm$ 1.0%
Energy Scale	$\pm$ 1.0%
PDF Uncertainty	$\pm$ 2.0%
Total	3.4 %

Table 21: Systematics on ZZ Acceptance

$$
\begin{array}{ll}
Z\text{+jets} & = 0.007 \pm 0.007 \text{ (stat.)} \pm 0.004 \text{ (syst.)} \\
Z\gamma\gamma & = 0.002 \pm 0.001 \text{ (stat.)} \pm 0.000 \text{ (syst.)} \pm 0.00 \text{ (lumi.)}
\end{array}
$$

The total background expectation for the ZZ search is

$$0.009 \pm 0.007 \pm 0.004.$$

8 Cross Section

The cross-section limit is calculated using a modified version of the technique suggested by Feldman and Cousins [12]. Their technique as does not allow for the uncertainty on the background estimate to be directly propagated into the confidence interval calculation. We have written a toy Monte Carlo based implementation of the Feldman-Cousin interval calculation that returns the same intervals as their paper for zero background uncertainty, but allows us to include the systematic uncertainty on the background estimate, acceptance and luminosity.

8.1 Details of the limit/interval calculator

The interval is calculated in two steps. Reading the Feldman and Cousins paper will help with the following explanation.

For each possible value of the cross-section, an acceptance interval is calculated. This is the range of possible observations which include 95% of the probability. There is choice for this interval (any set including 95% is statistically valid). We follow the Feldman-Cousins ranking procedure. The acceptance interval is determined by toy Monte Carlo. We generate a set of Poisson experiments in which the prediction is varied based on the systematic uncertainties. The prediction inputs are the luminosity-dependent background, $B_{\mathrm{lumi-dep}}$, the luminosity-independent background, $B_{\mathrm{lumi-indep}}$, the acceptance, A, and the luminosity, $\mathcal{L}$. The calculation is then

$$N_{\mathrm{expected}} \quad = \quad \tilde{A}\tilde{\mathcal{L}}\sigma + \frac{\tilde{\mathcal{L}}}{\mathcal{L}}\tilde{B}_{\mathrm{lumi-dep}} + \tilde{B}_{\mathrm{lumi-indep}}, \tag{5}$$

where $\tilde{}$ denotes the varied version of the variable and σ is the cross-section for which the acceptance interval is being calculated. The range including the top 95% of the ranked experiments is the acceptance interval.

The confidence interval is then the range possible values of the cross-section for which the acceptance interval includes the number of observed events.

We have preformed two cross-checks of implementation. First the systematic uncertainties were set to zero and the results were compared with the **TFeldmanCousins** ROOT class. The second check with the full systematics is that 95% of experiments produce intervals which contain the generate cross-section.

Variable	Source	Value
$B_{\mathrm{lumi-dep}}$	$Z\gamma + ZZ + t\bar{t}$	1.43±0.20
$B_{\mathrm{lumi-indep}}$	Z+jets	1.21±0.39
$\mathcal{L}$	1100.9×(1±0.06)	1100.9±66.1
A	0.134×0.0180×(1±0.04)	0.002412±0.000096

Table 22: Inputs to WZ cross-section calculation.

8.2 Cross-section Results

The final results are $5.00^{+1.81}_{-1.59}$ pb with systematics. For comparison both the cross-section calculator and TFeldmanCousins give $5.00^{+1.81}_{-1.38}$ pb. The number input into Equation 5 for the calculation are shown in Table 22.

We use the same procedure for the ZZ analysis. We find a cross-section bound of $[0.035, 3.8]$ pb with systematics and $[0.033, 3.8]$ pb without systematics. Because the lower bound is very close to zero, we will describe the results as a limit of $\sigma(ZZ) < 3.8$ pb. We feel that this bound along with the significance of value of 2.6σ correctly represents the result.

9 Summary and Conclusions

We have searched for WZ and ZZ production in the 1.1fb^{-1} dataset.

In the WZ analysis, we expect

$$9.75 \pm 0.03(stat.) \pm 0.31(syst.) \pm 0.59(lumi.)$$

events of signal and

$$2.65 \pm 0.28(stat.) \pm 0.33(syst.) \pm 0.09(lumi.)$$

We observe 16 WZ candidate events. Comparing a Maximum Likelihood fit in two bins of MET with expectations from background only, we find that 2 in a Billion background only experiments results in an ML fit significance as large as the one observed in data. This is equivalent to the one sided 5.9σ tail of a Gaussian distribution. This is the first observation ($> 5\sigma$) of WZ production.The measured cross section is

$$\sigma(WZ) = 5.0^{+1.8}_{-1.6}\ (\mathrm{stat.} + \mathrm{syst.})\ \mathrm{pb}$$

consistent with the next to leading order SM prediction of 3.7 ± 0.3 pb. Both the cross-section and the two binned $\not\!\!E_T$ distribution used to assess the significance are consistent with the standard model expectations.

In the ZZ search, we expect

$$1.884 \pm 0.015 \text{ (stat.)} \pm 0.061 \text{ (syst.)} \pm 0.113 \text{ (lumi.)}$$

events of signal and

$$0.009 \pm 0.007 \text{ (stat.)} \pm 0.004 \text{ (syst.)} \pm 0.0005 \text{ (lumi.)}$$

events of background. We observe one 4 muon ZZ candidate, which corresponds to a 2.6 σ significance, based on which we set a limit of $\sigma(ZZ) < 3.8$ pb which is consistent with the NLO prediction of 1.39 ± 0.1 pb.

A Dilepton Control Region - Detailed

This section shows some kinematic plots in the dilepton control region, broken down by dilepton category.

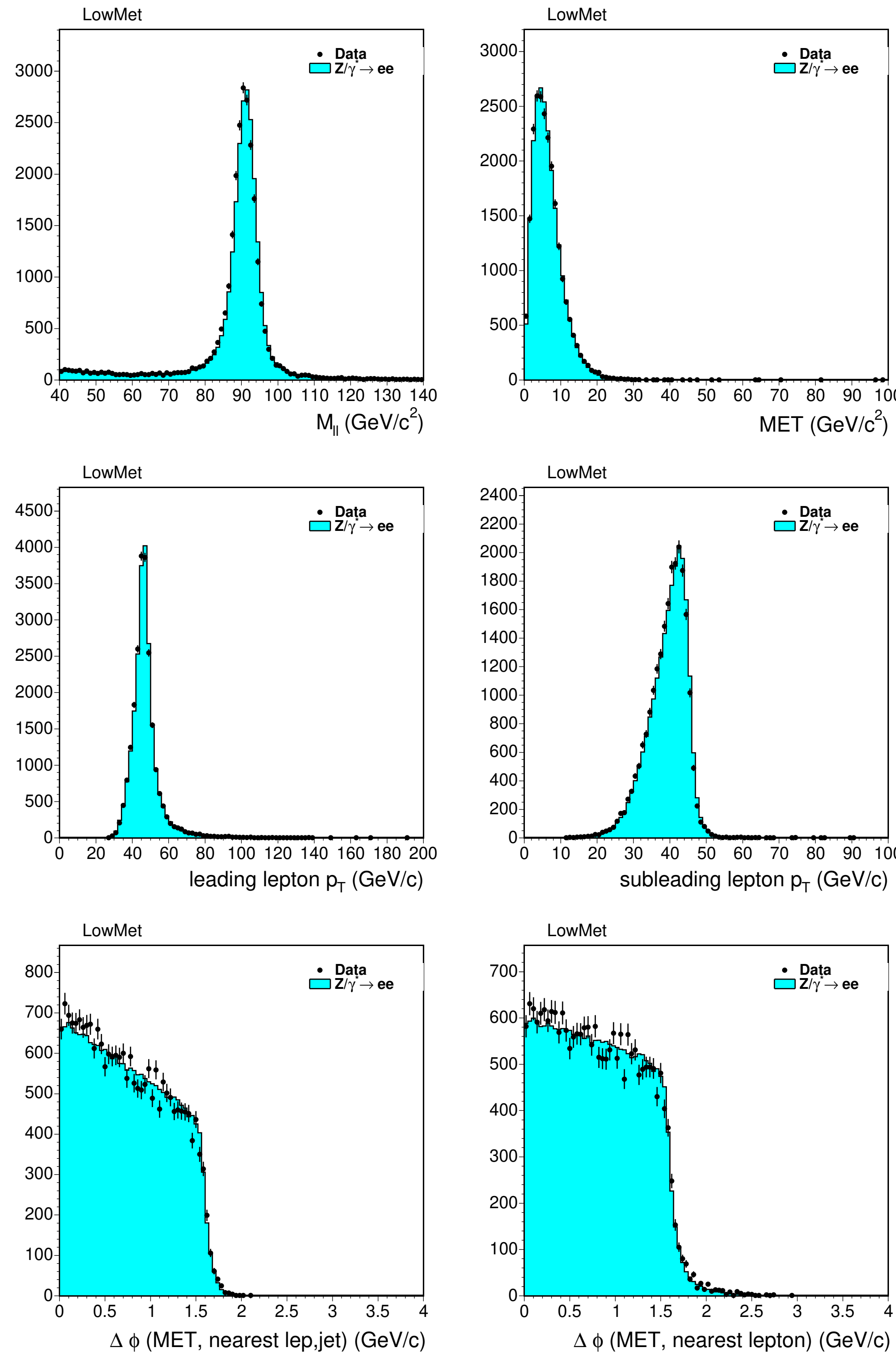

Figure 25: Drell-Yan ($Z \to e^+e^-$) control region **(TCE-TCE)**

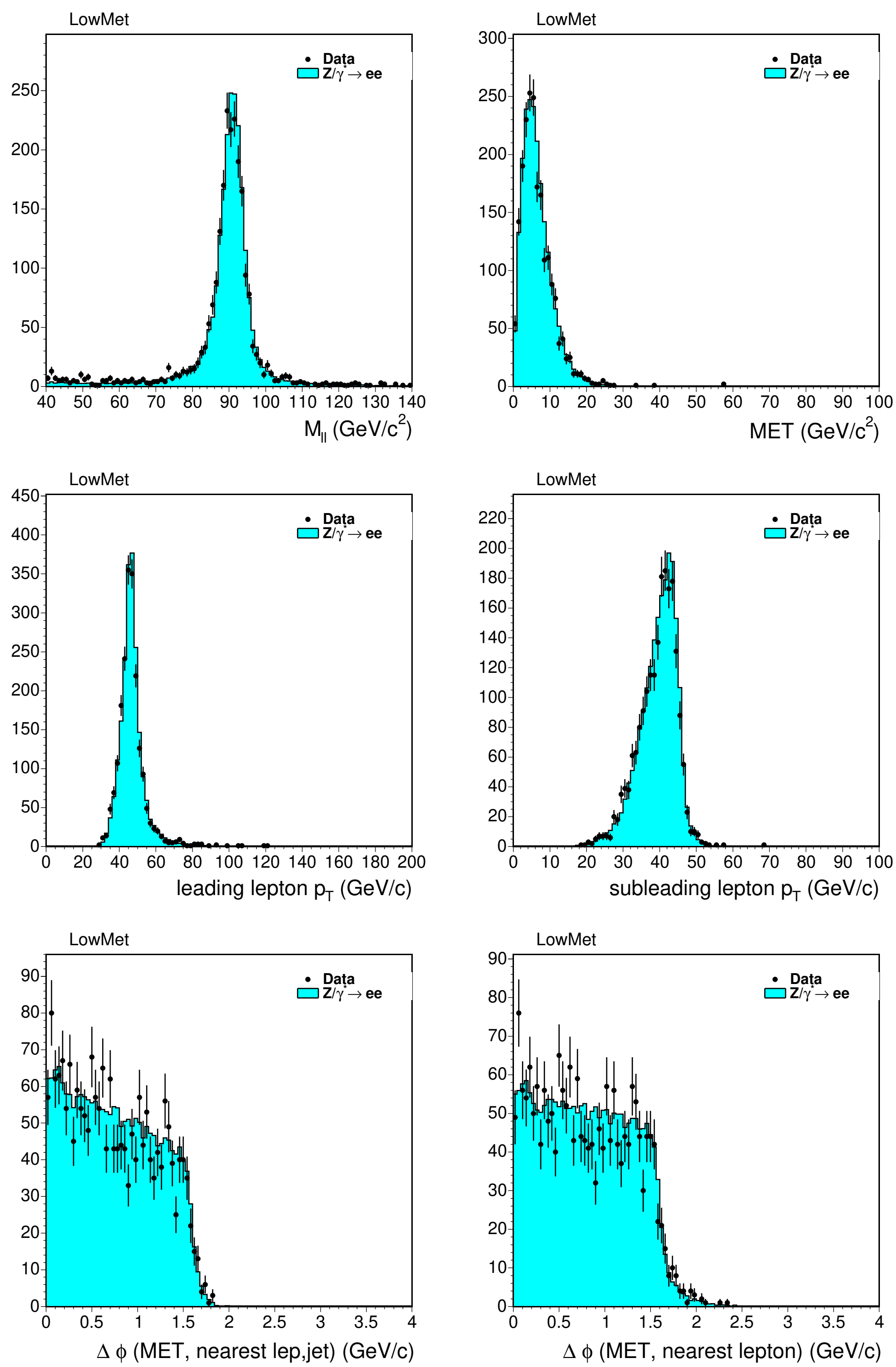

Figure 26: Drell-Yan ($Z \to e^+e^-$) control region **(TCE-LCE)**

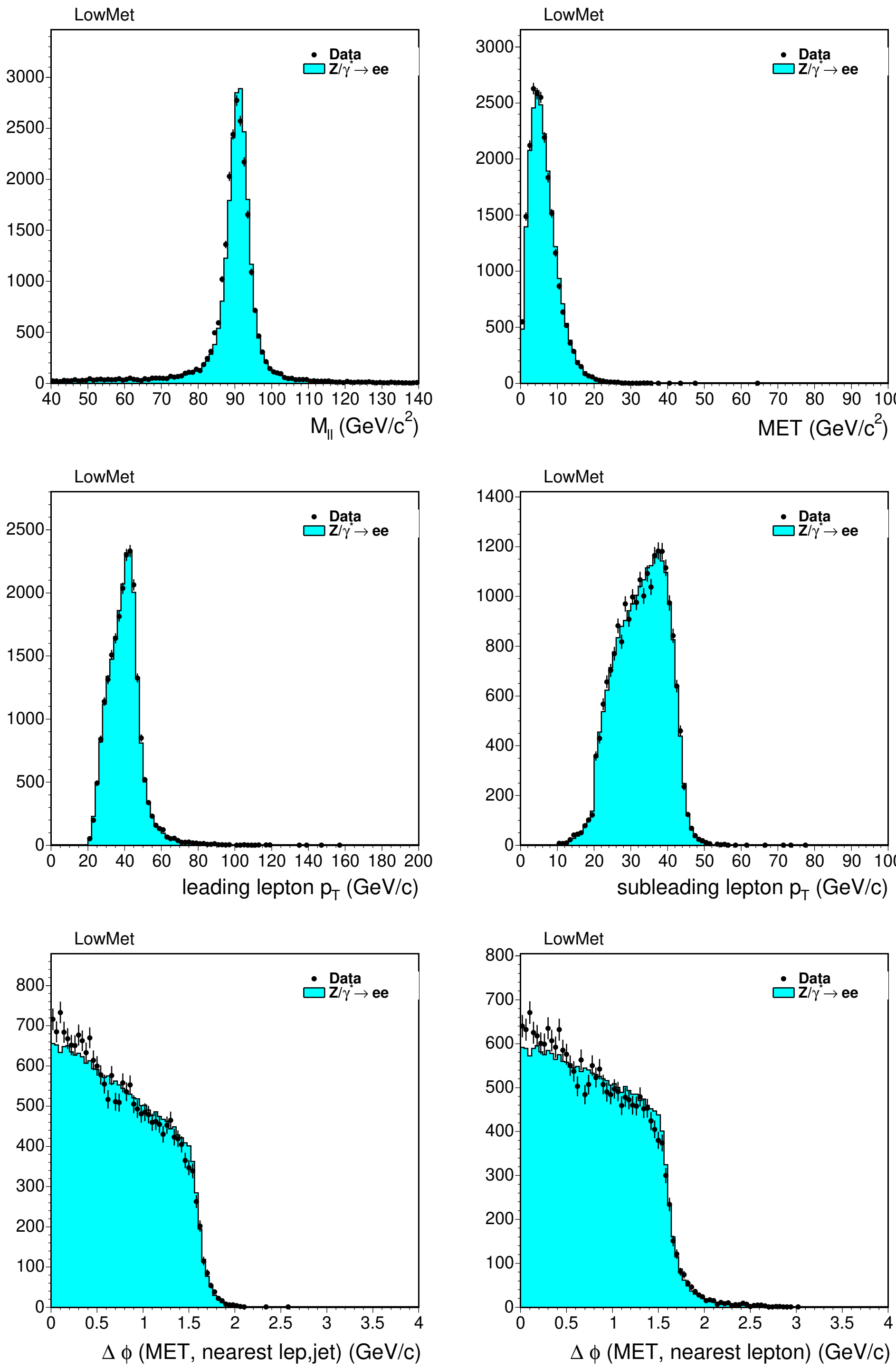

Figure 27: Drell-Yan ($Z \rightarrow e^+e^-$) control region **(TCE-PHX)**

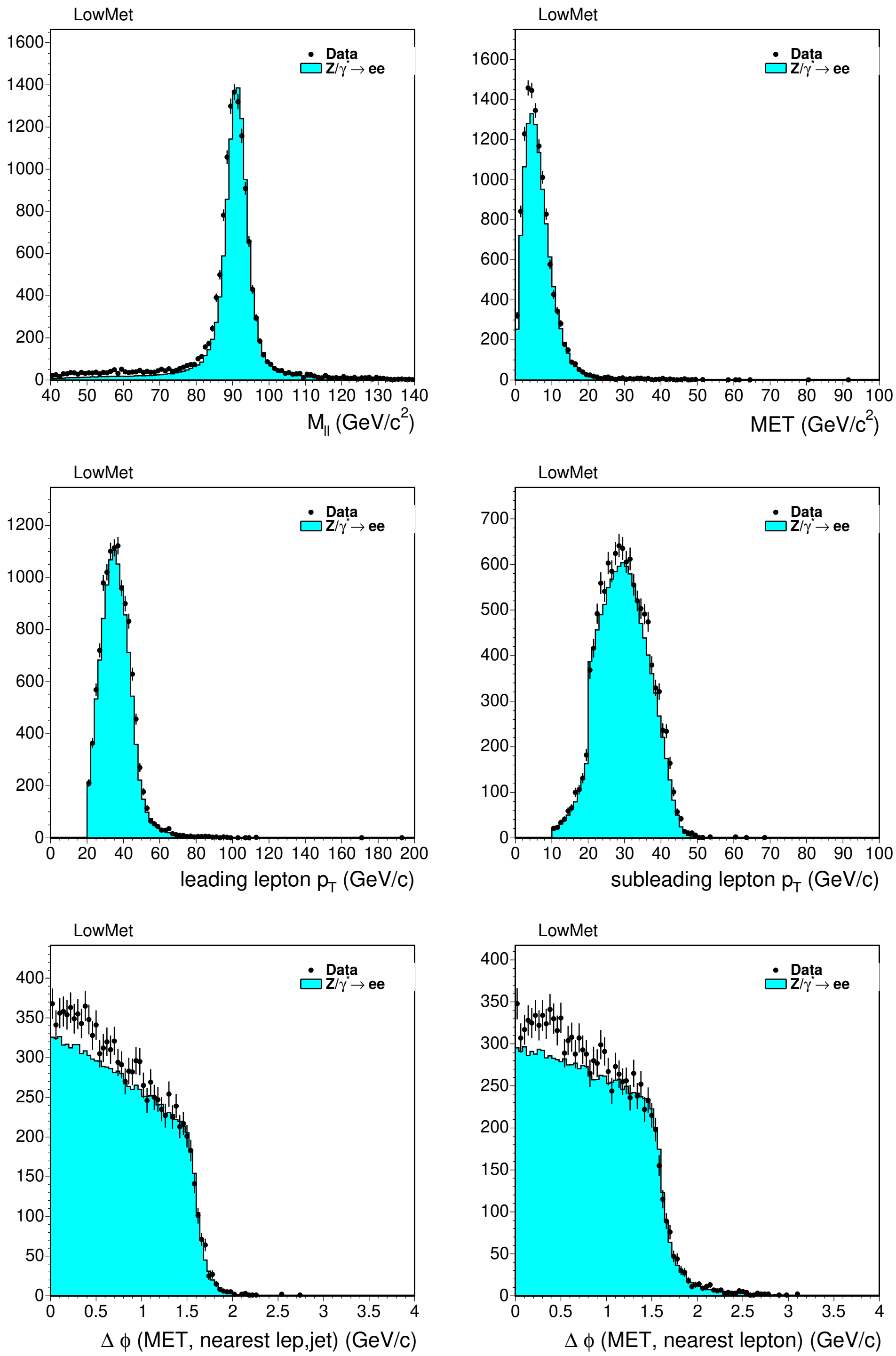

Figure 28: Drell-Yan ($Z \to e^+e^-$) control region **(TCE-PEM)**

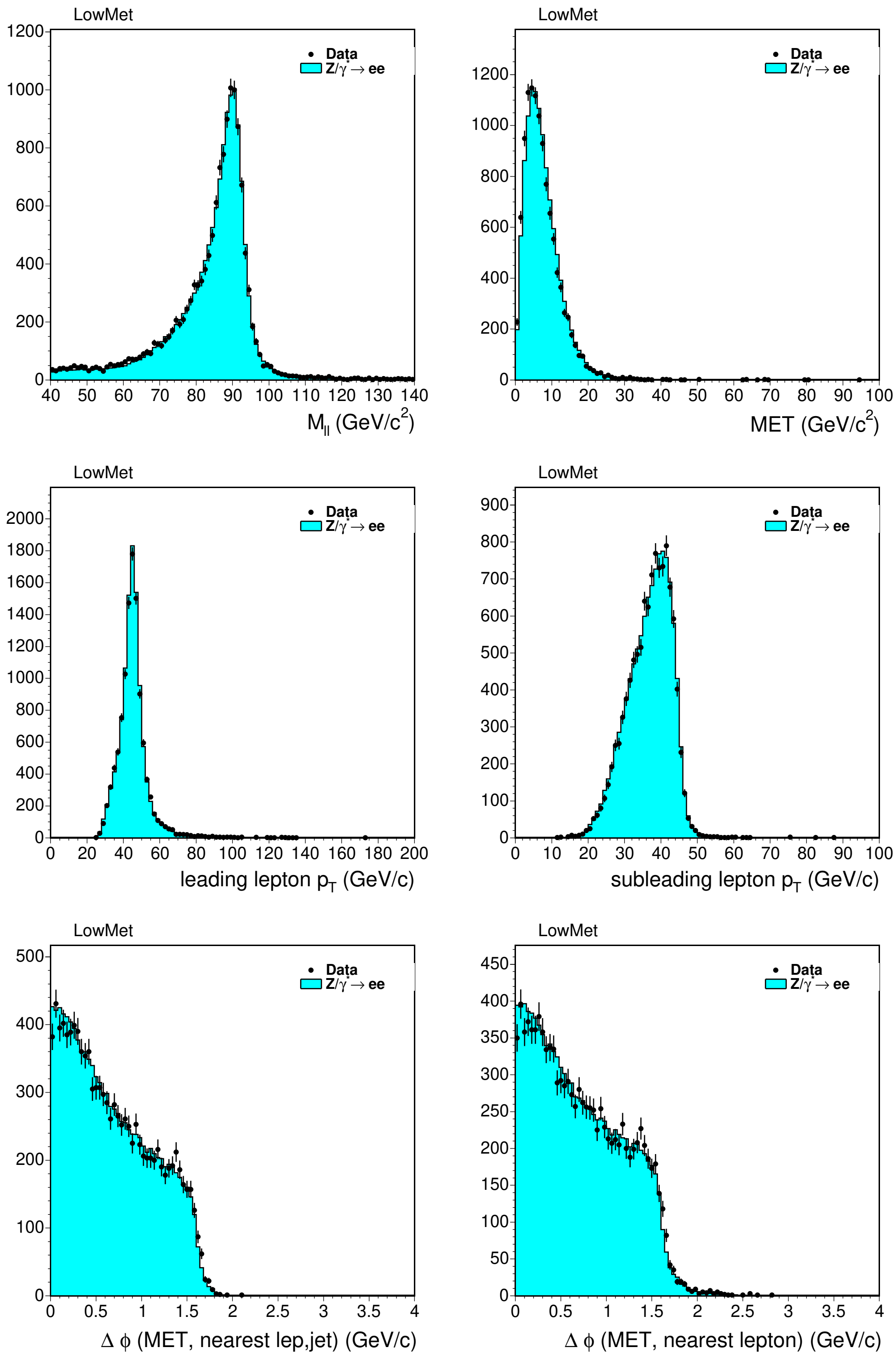

Figure 29: Drell-Yan ($Z \rightarrow e^+e^-$) control region **(TCE-CrkTrk)**

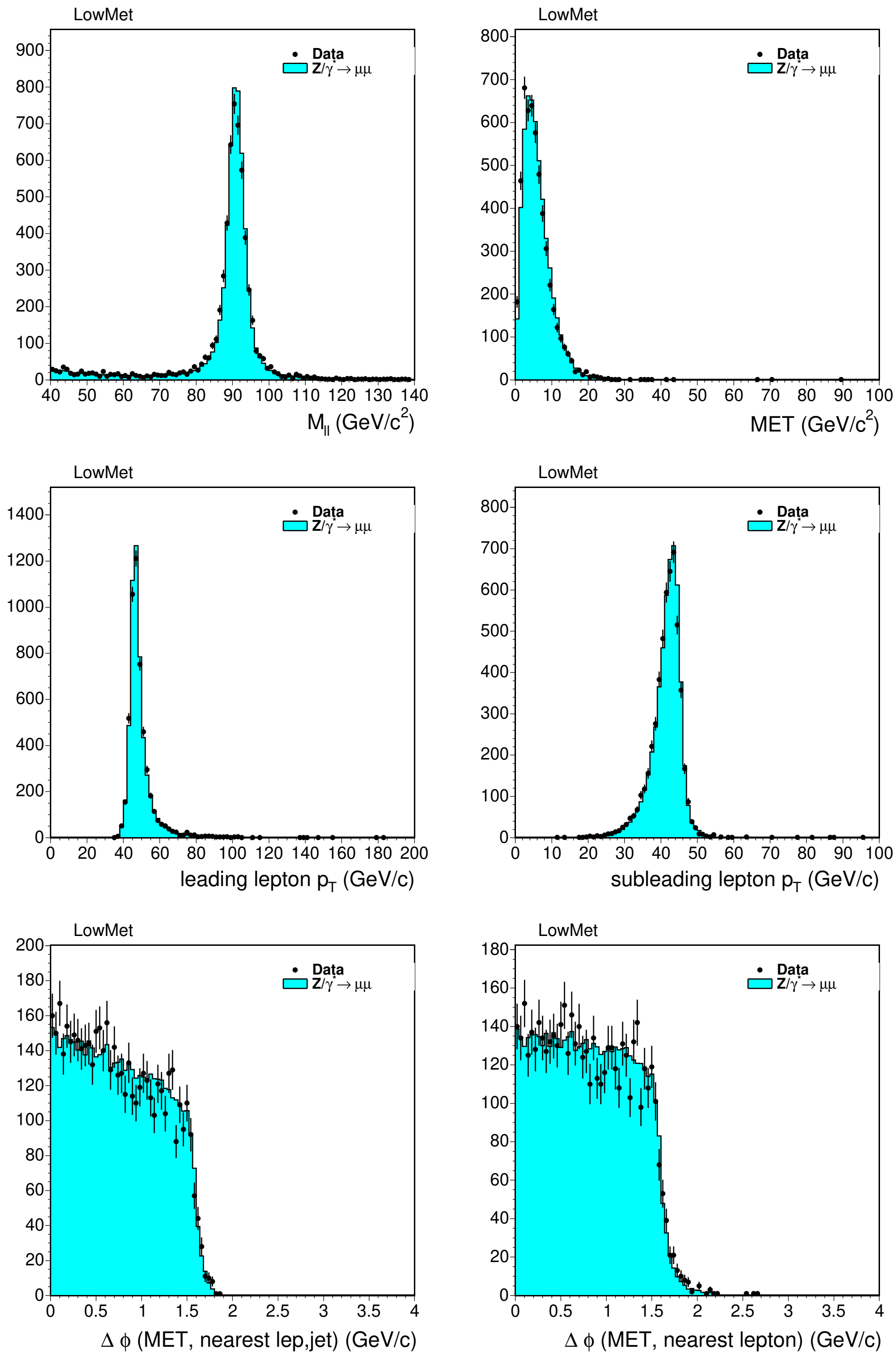

Figure 30: Drell-Yan ($Z \rightarrow e^+e^-$) control region **(CMUP-CMUP)**

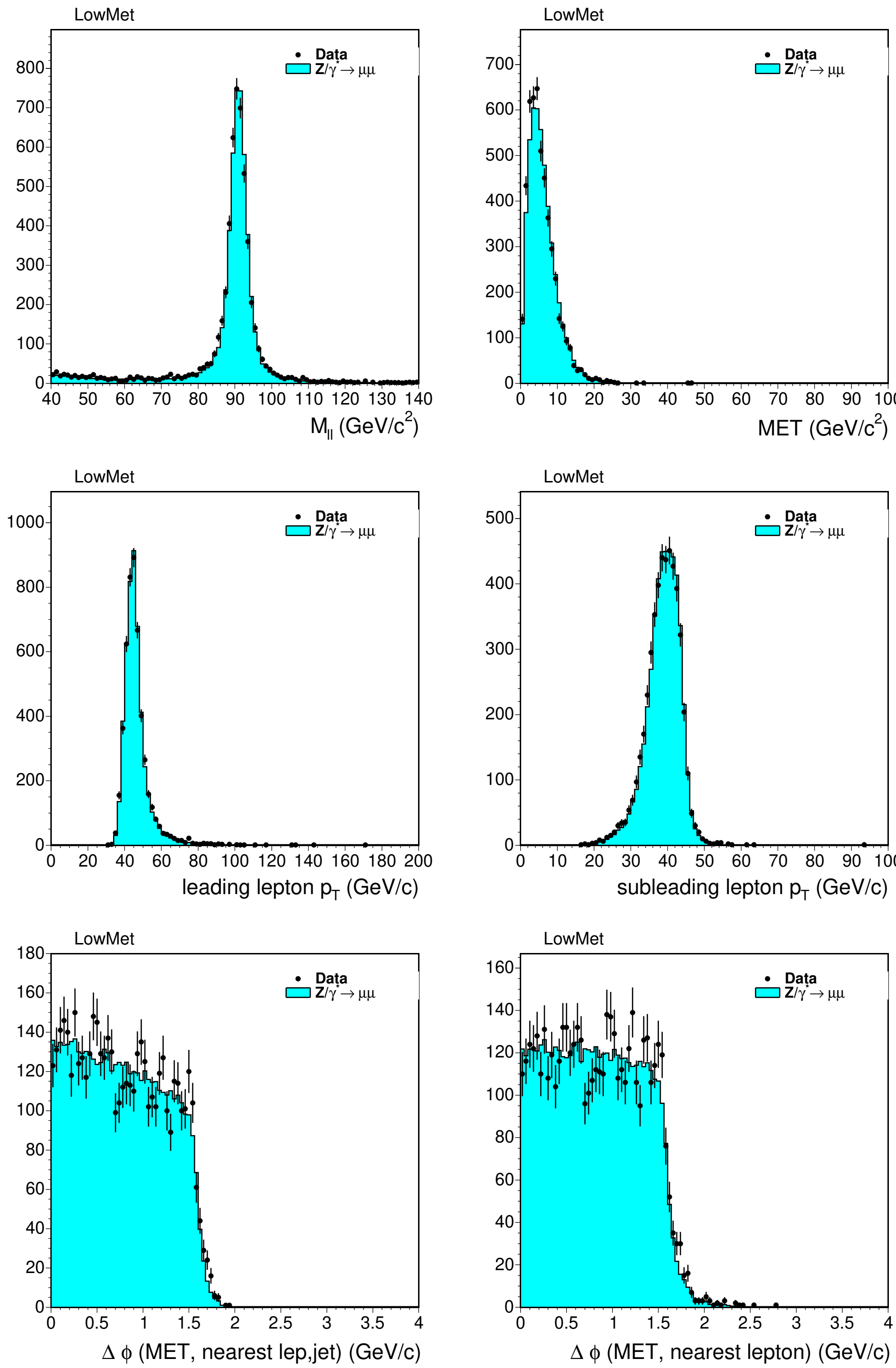

Figure 31: Drell-Yan ($Z \rightarrow e^+e^-$) control region **(CMUP-CMX)**

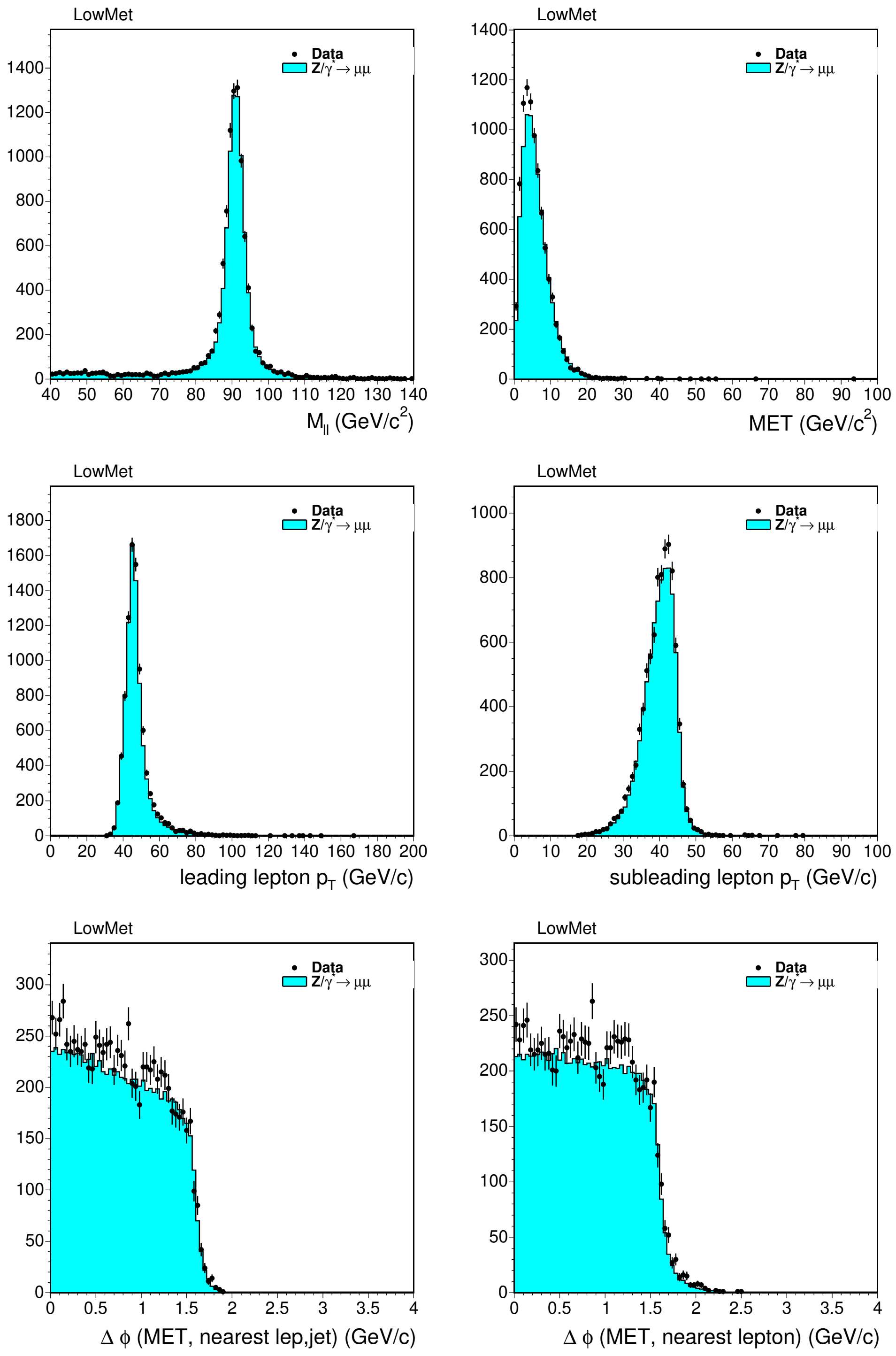

Figure 32: Drell-Yan ($Z \rightarrow e^+e^-$) control region **(CMUP-CMIOCES)**

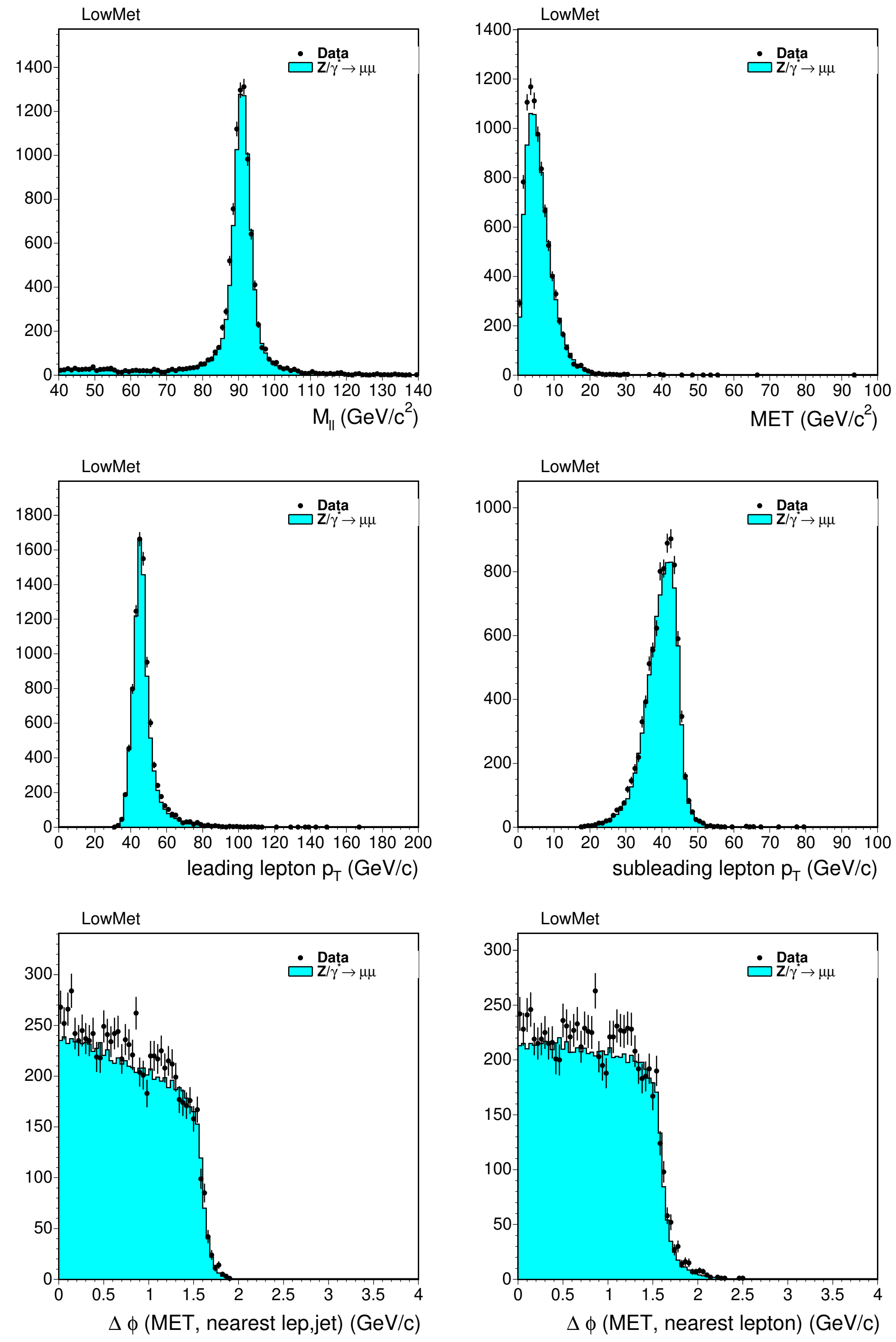

Figure 33: Drell-Yan ($Z \to e^+e^-$) control region **(CMUP-CMIOPES)**

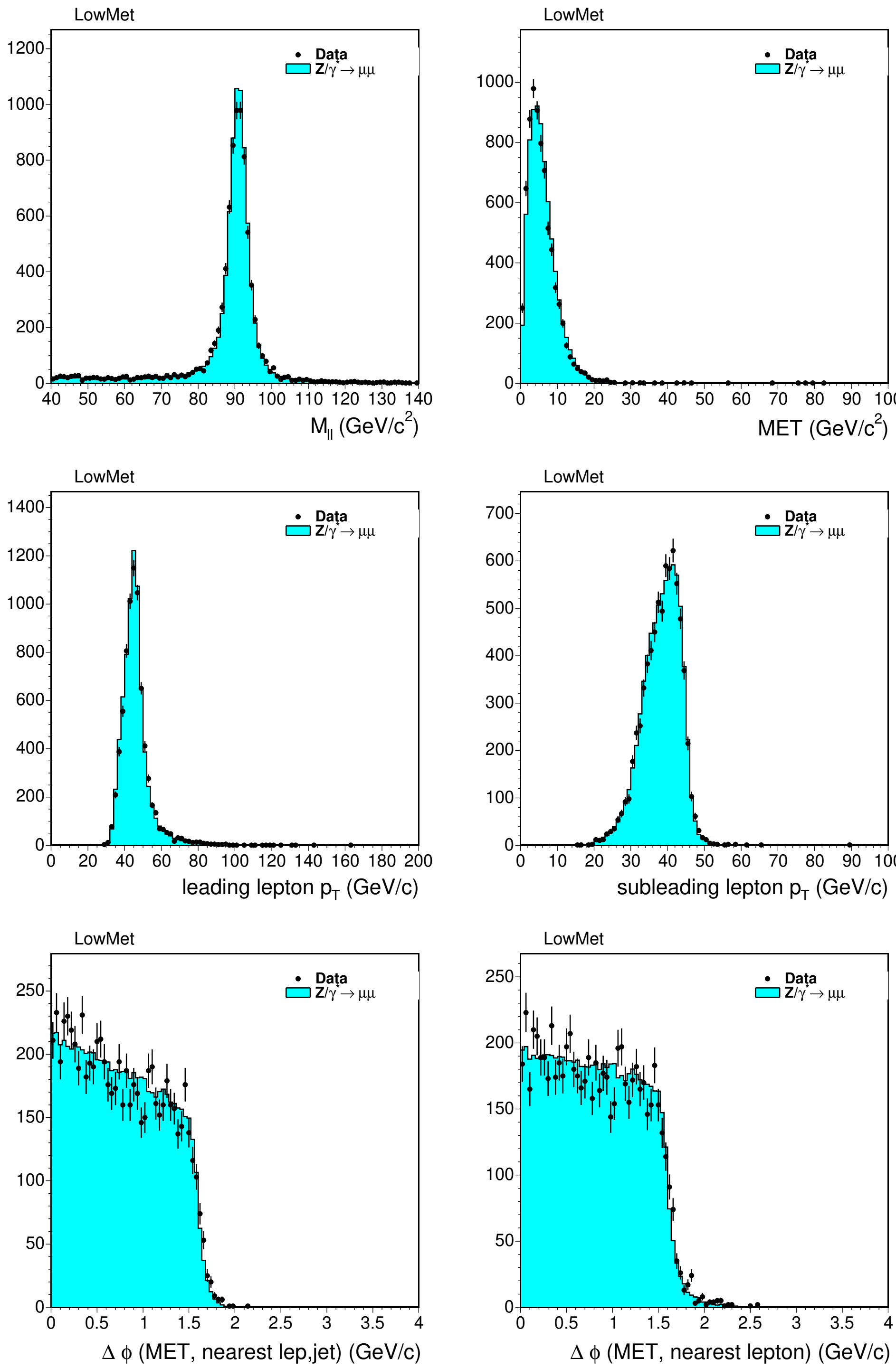

Figure 34: Drell-Yan ($Z \to e^+e^-$) control region **(CMUP-CrkTrk)**

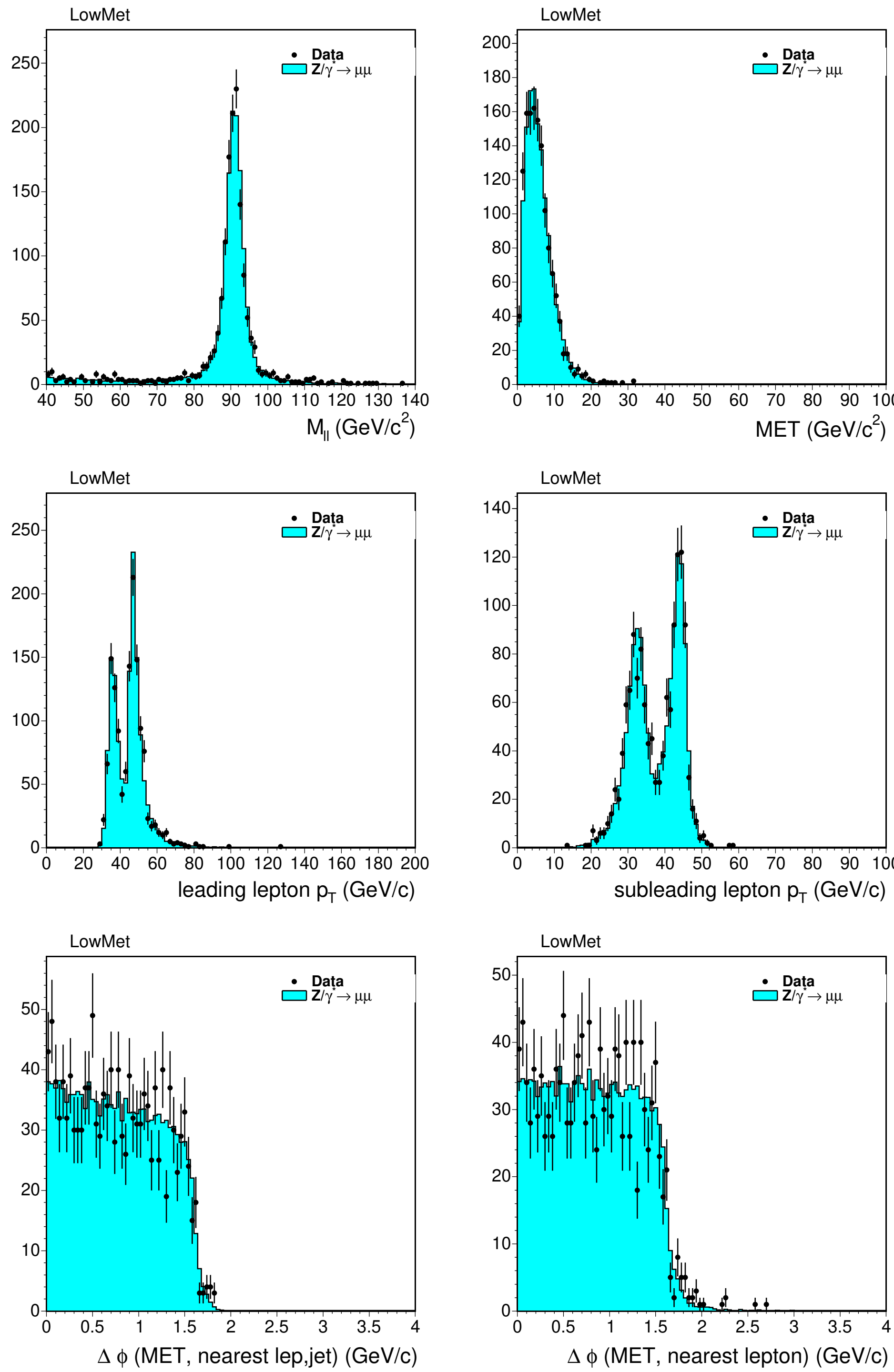

Figure 35: Drell-Yan ($Z \to e^+e^-$) control region **(CMX-CMX)**

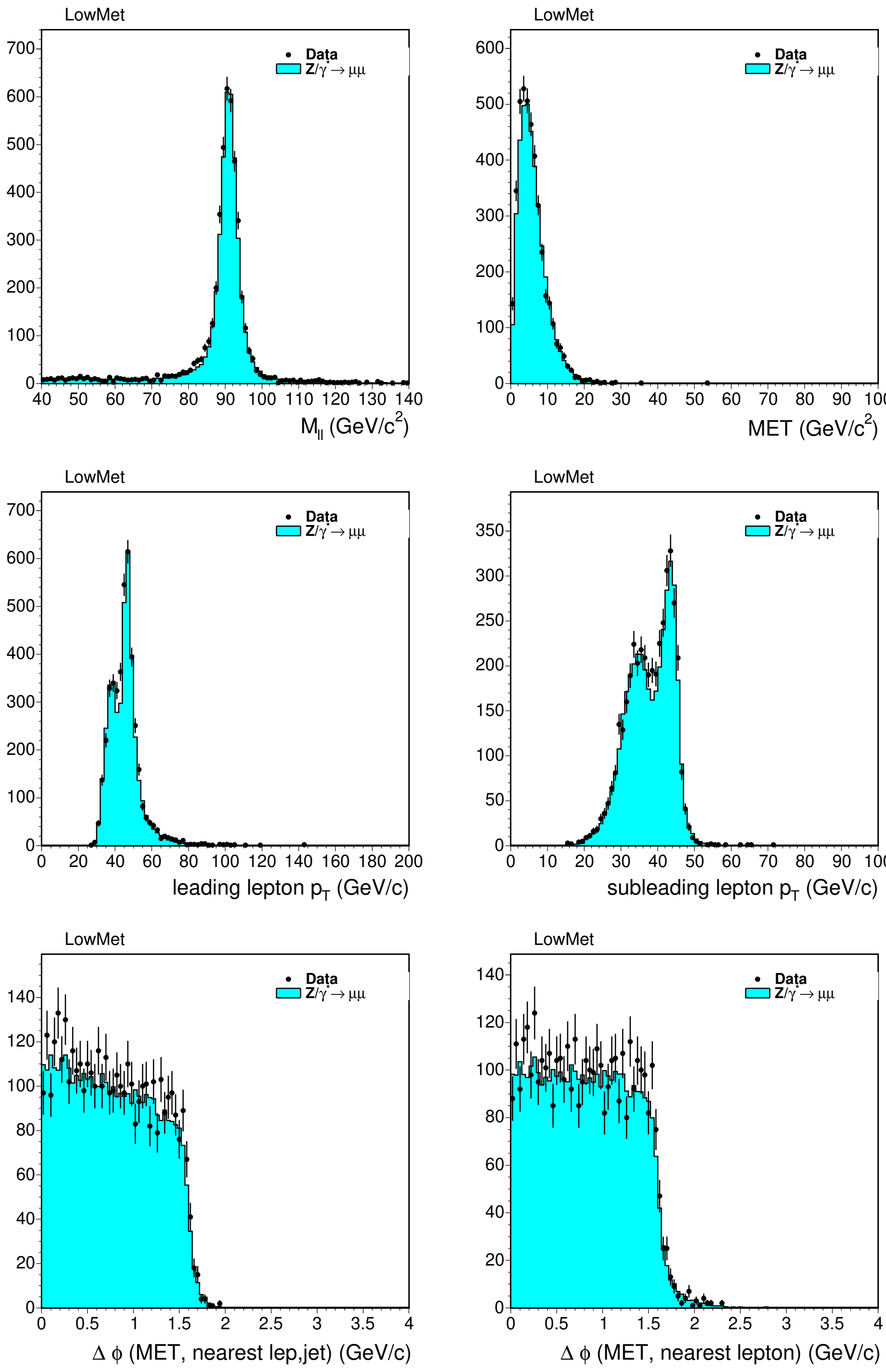

Figure 36: Drell-Yan ($Z \to e^+e^-$) control region **(CMX-CMIOCES)**

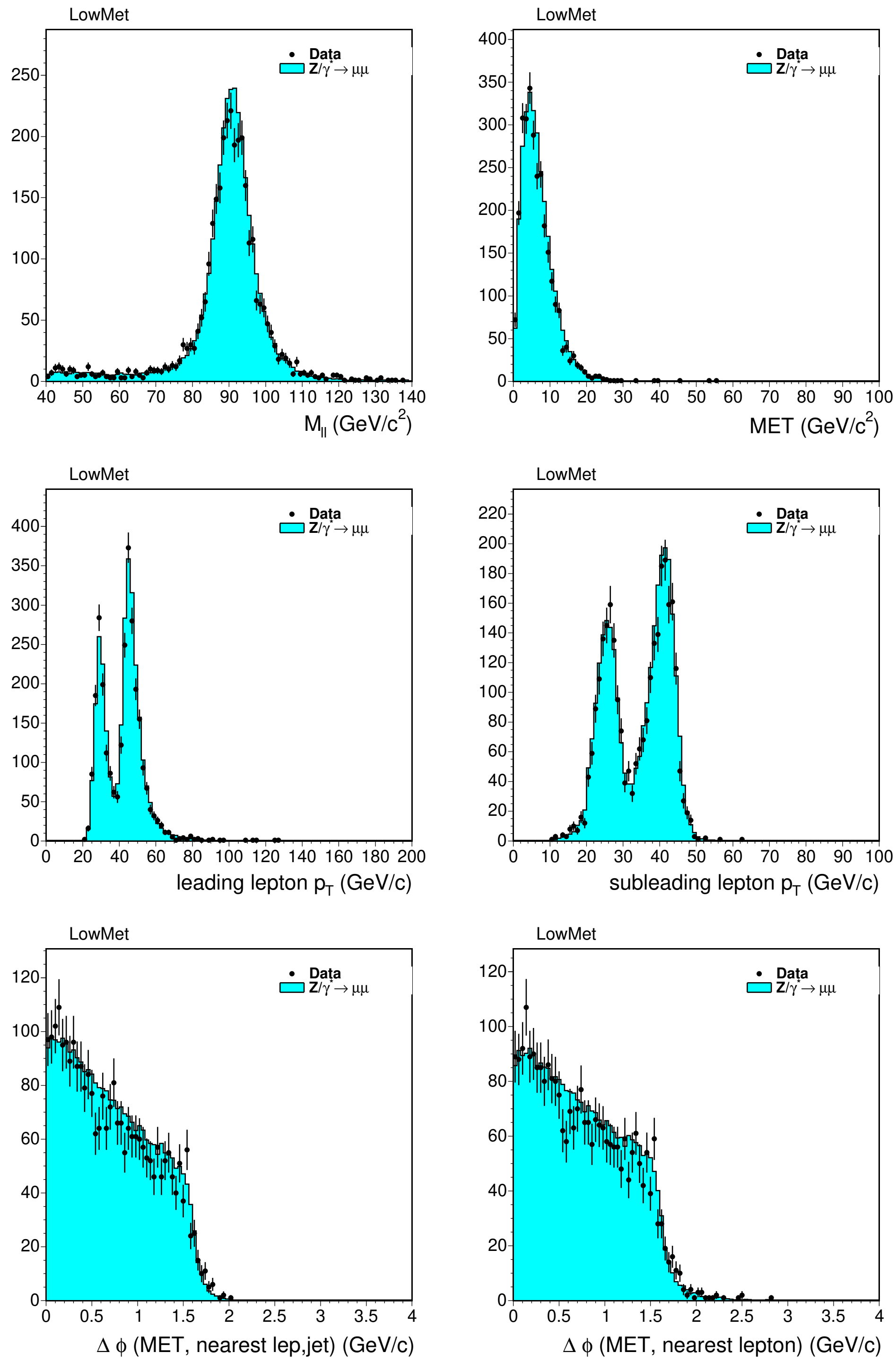

Figure 37: Drell-Yan ($Z \rightarrow e^+e^-$) control region **(CMX-CMIOPES)**

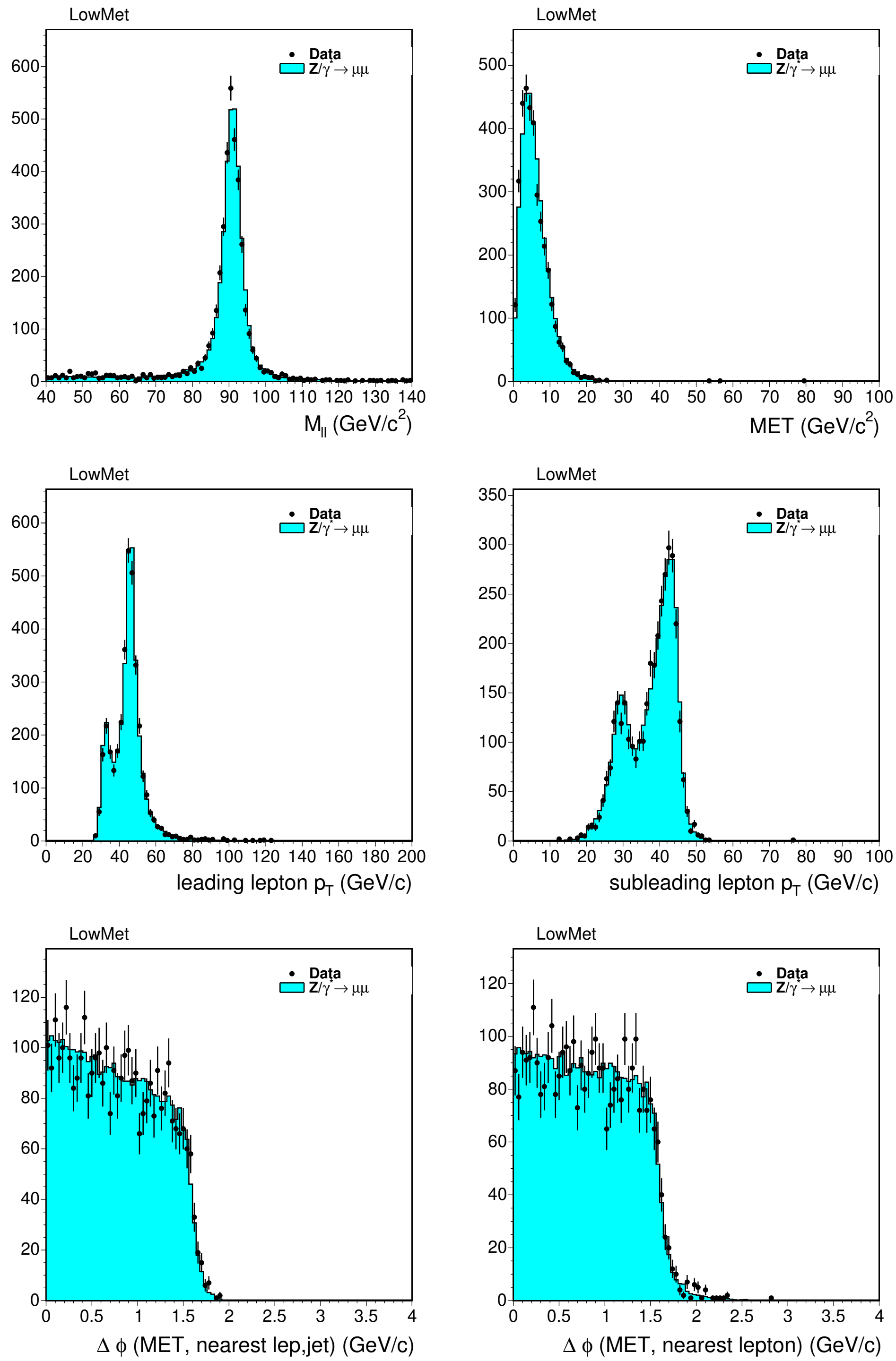

Figure 38: Drell-Yan ($Z \to e^+e^-$) control region **(CMX-CrkTrk)**

References

[1] J. M. Campbell and R. K. Ellis, Phys. Rev. **D60**, 113006 (1999), `hep-ph/9905386`.

[2] D. Acosta et al. (CDF), Phys. Rev. **D71**, 091105 (2005), `hep-ex/0501021`.

[3] S. Hsu, E. Lipeles, K. McCarthy, M. Neubauer, and F. Wurthwein, *Measurement of the wz cross section in trileptons + missing transverse energy* (2006), CDF/ANAL/EWK/CDFR/8095.

[4] V. Boisvert, *Trigger efficiencies for the high et central electrons in gen6* (2006), CDF/DOC/ELECTRON/CDFR/7939.

[5] B. Han and E. Halkiadakis, *Met pem trigger efficiency for pheonix electrons* (2006), CDF/DOC/ELECTRON/CDFR/7940.

[6] S. Cabrera, J. Deng, G. A., C. Hays, Y. Huang, and M. Kruse, *Measurement of the zz + zw cross section using run ii data* (2004), CDF/ANAL/ELECTROWEAK/GROUP/6920.

[7] U. Baur and E. L. Berger, Phys. Rev. **D47**, 4889 (1993).

[8] S. Hsu, E. Lipeles, M. Neubauer, F. Wurthwein, and R. Vanguri, *Lepton id for multilepton diboson analyses* (2006), CDF/ANAL/EWK/CDFR/8538.

[9] A. Attal and A. Canepa, *Photon conversion removal efficiency* (2006), CDF/ANAL/ELECTRON/CDFR/8073.

[10] S. Hsu, E. Lipeles, K. McCarthy, M. Neubauer, and F. Wurthwein, *Lepton id and fake rates for the ww and wz analyses* (2006), CDF/ANAL/EWK/CDFR/8093.

[11] S. Hsu, E. Lipeles, K. McCarthy, M. Neubauer, and F. Wurthwein, *Measurement of the ww cross section using 0.8*fb^{-1} (2006), CDF/ANAL/EWK/CDFR/8094.

[12] G. J. Feldman and R. D. Cousins, Phys. Rev. D **57**, 3873 (1998).